Appendix B Response to Coherency Issues from the Oct 24, 2006 Meeting

At the Oct 24, 2006 coherency review meeting, the following items were identified as critical issues that needed to be addressed to complete the review of the coherency model:

1. Correct the timing/polarity of the Pinyon Flat data so that this data can be used to check the plane-wave coherency model for a hard-rock site.

2. Develop a revised coherency model for the coherency for embedded structures.

3. Evaluate the correlation of the FAS and the coherency

4. Check the magnitude dependence at higher frequency

5. Separate the EPRI Parkfield events and use the one with the better signal to noise at high frequencies (> 20 Hz)

6. Provide the EPRI proprietary coherency model report

7. Provide the digital data base used to develop the coherency model

Items 1-5 are addressed in this appendix. The remaining two items are addressed separately.

Item 1. Pinyon Flat Data

Some of the pane-wave coherencies computed from the Pinyon Flat data were unusually low, indicating that there may be a problem with either the timing or the polarity of some of the recordings. This would not affect the lagged coherency because taking the modulus of the complex coherency removes any effect of polarity or small timing errors.

The recordings from the five Pinyon Flat events were examined to determine if there are any polarity error. To examine the problem of polarity reversal and other data problems, each velocity component was integrated to displacement and band-pass filtered between 0.2 and 1 Hz using a 2nd order causal (zero phase) Butterworth filter. The errors found for each event are summarized below.

The P-wave arrival time was also measured for each station to allow the recordings to be aligned on the P-wave which removes timing errors. Before picking the arrival time, the D.C. level of a vertical component was removed and an 8th-order causal (zero phase) Butterworth low-pass filter with a 40Hz corner frequency was then applied to the vertical component. The steep filter roll-off is intended to remove the 60-Hz noise that sometimes interferes with the picking of arrival time. The selected P-wave arrival times are listed below.

The P-wave arrival times are used to align the data to correct the timing. The figures show that there is are large difference in the P-wave arrival times (up to 0.2 sec) that indicate timing errors.

With these corrections to the polarity and timing, these data can be used to compare to the plane-wave coherency model. (See below and Item 3).

Event PF 90.108.14.25.58

For this event, the following problems were found:

	Problem	Resolution
1	*x03y15_e* is identical to *x03y15_n*. The real *x03y15_e* is in *x03y15_z*.	File name is corrected
2	As stated above, record *x03y15_z* is actually *z03y15_e*. The real *x03y15_z* is in *x03y08_n*.	File name is corrected
3	Data in *x03y08_n* is actually data for *x03y15_z*. The real *x03y08_n* is missing.	File name is corrected
4	Polarity of *x01y00_e* is reversed.	Polarity is corrected
5	Quality of *x03y14_n* is questionable. It has a waveform quite different from other N-component records.	Recording x03y14_n is excluded.
6	Quality of *x12y03_n* is questionable. It has a waveform quite different from other N-component records.	Recording x12y03_n is excluded.

Figure 1-1 shows the 41 Pinyon Flat Array stations that recorded the 1990 April 18 14:25:58 event. The arrival times of the first P wave on the vertical component are listed in Table 1-1 and plotted in Figure 1-2 for each of the 41 records. The timing error is up to about 0.2 sec.

The displacement records, after aligning the records on the P-wave, are shown in Figure 1-3.

Table 1-1. P-Wave Arrival Time of Event PF_90.108.14.25.58

	File Name	Station-East (m)	Station-North (m)	Station-Z	P-wave Arrival Time (sec)
2	x00y00_z	-4.97	15.78	-0.77	8.71592
3	x00y01_z	-5.11	9.21	-2.18	8.77099
4	x00y02_z	-6.42	1.52	-1.83	8.59094
5	x00y04_z	-6.14	-11.59	-2.44	8.73411
6	x00y05_z	-6.70	-18.57	-3.10	8.68240
7	x01y00_z	1.82	15.39	-1.03	8.71526
8	x01y01_z	1.51	9.15	-0.93	8.77242
9	x01y02_z	1.02	2.38	-1.14	8.59237
10	x01y04_z	0.55	-11.67	-2.34	8.73098
11	x01y05_z	0.22	-18.89	-3.27	8.68097
12	x02y00_z	8.24	15.44	0.19	8.68382
13	x02y01_z	9.03	9.49	-0.55	8.48376
14	x02y02_z	7.72	2.08	-1.30	8.45818
15	x02y04_z	7.22	-11.60	-2.34	8.69954
16	x03y00_z	14.96	16.25	-0.34	8.68382
17	x03y01_z	15.10	8.75	-0.97	8.48376
18	x03y02_z	14.70	2.18	-1.44	8.45518
19	x03y04_z	14.50	-11.69	-2.50	8.69811
20	x03y06_z	14.25	-32.35	-4.30	8.67096
21	x03y08_z	10.99	-73.11	-6.52	8.70812
22	x03y09_z	12.13	-93.75	-7.61	8.73527
23	x03y11_z	9.84	-134.80	-10.42	8.60952
24	x03y12_z	9.30	-155.39	-11.38	8.68382
25	x03y13_z	8.14	-176.24	-12.54	8.60952
26	x03y14_z	7.27	-198.16	-14.15	8.63667
27	x03y15_z	7.78	-218.32	-15.85	8.71383
28	x03y16_z	4.87	-239.05	-17.97	8.63810
29	x04y00_z	21.89	16.20	-0.63	8.65810
30	x04y01_z	21.89	8.84	-0.60	8.72241
31	x04y02_z	21.57	2.18	-1.34	8.69469
32	x04y03_z	21.05	-4.61	-1.69	8.54235
33	x05y00_z	29.20	15.69	-0.85	8.65810
34	x05y01_z	28.93	9.31	-0.45	8.72384
35	x05y02_z	28.65	2.17	-1.00	8.69240
36	x05y03_z	28.55	-4.65	-1.28	8.54092
37	x06y03_z	42.69	-4.65	-1.48	8.72527
38	x11y03_z	146.85	-3.07	-1.34	8.51663
39	x12y03_z	167.69	-2.47	0.07	8.51234
40	x15y03_z	229.52	-2.66	0.41	8.66239
41	x16y03_z	250.13	-4.51	0.96	8.66286

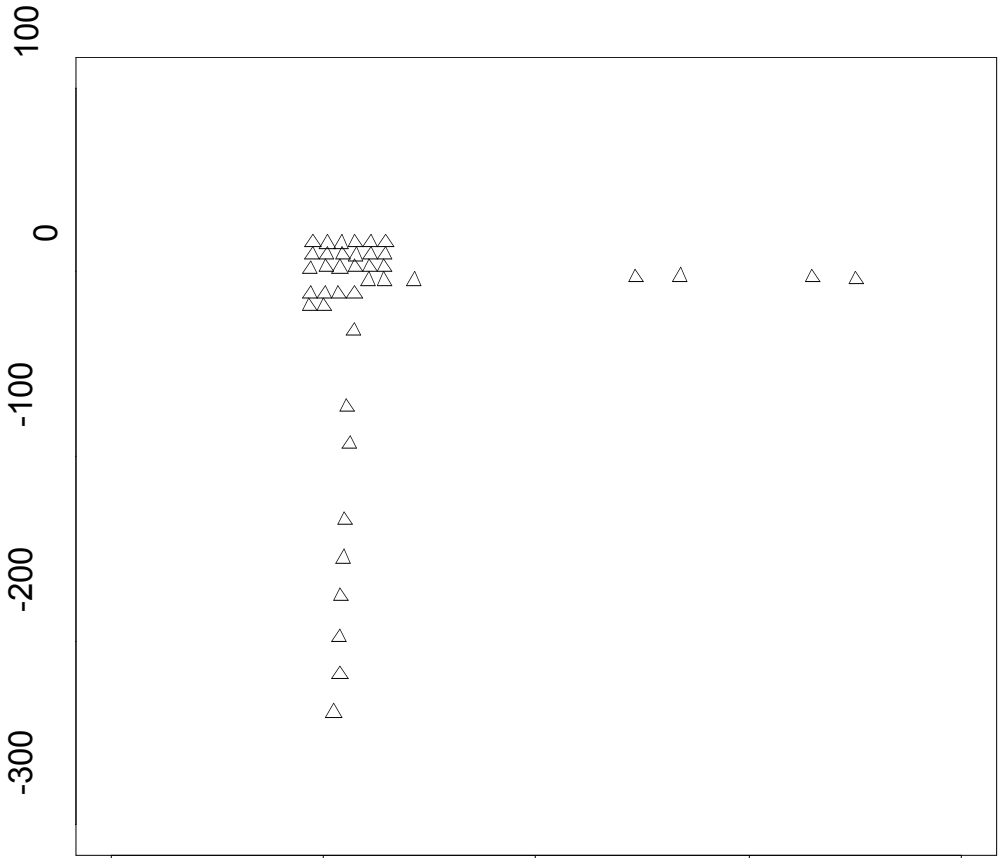

Figure 1-1. Location of stations that recorded event PF_90.108.14.25.58.

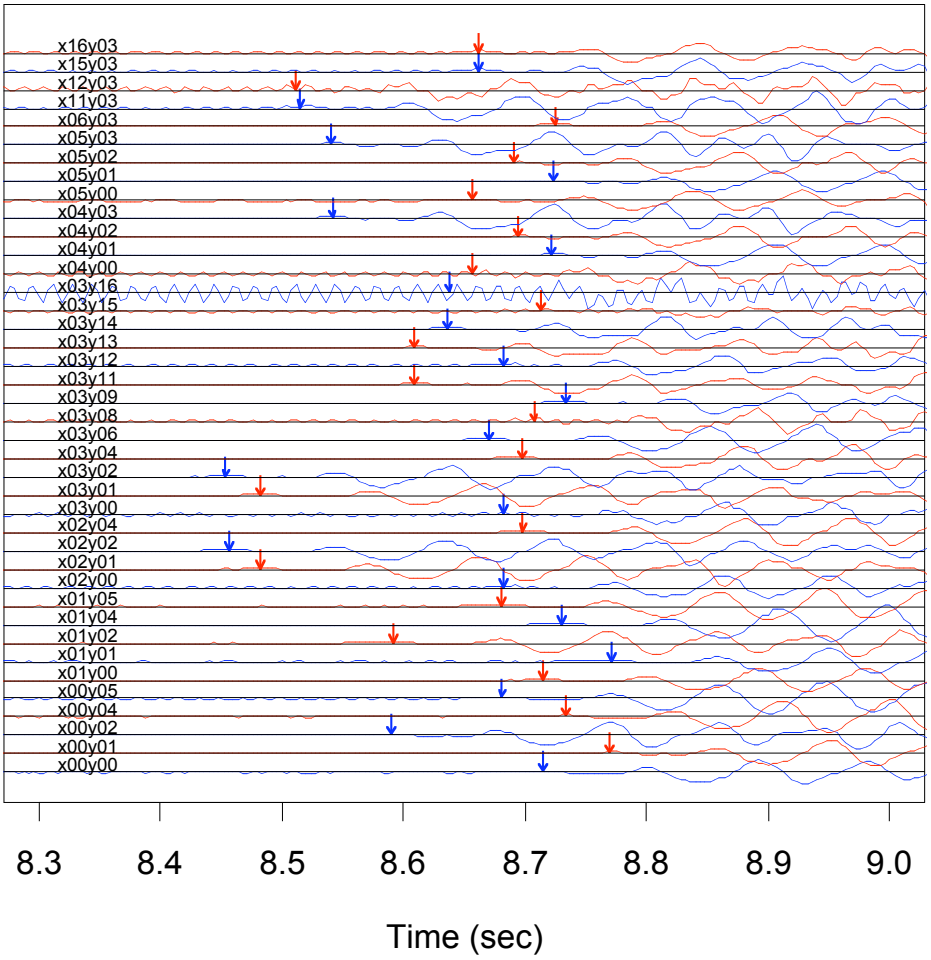

Figure 1-2. Velocity time histories of the Z-component for PF_90.108.14.25.58. The arrows indicate the picked arrival times.

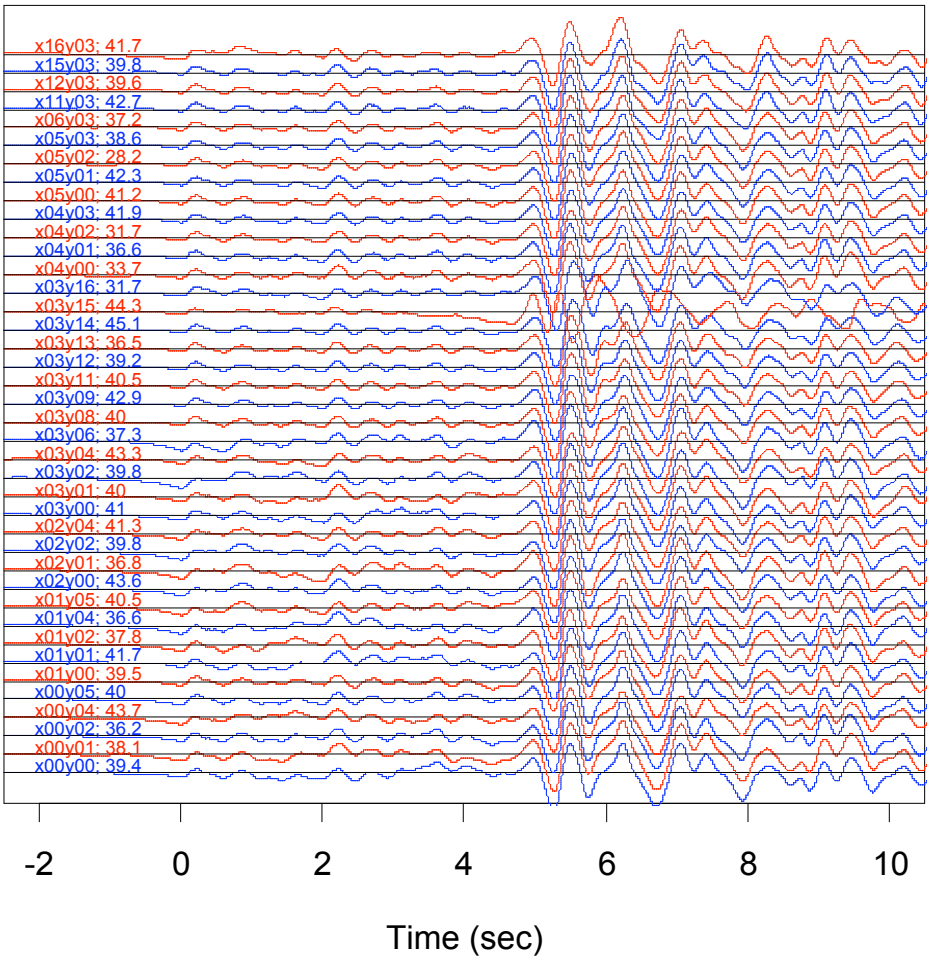

Figure 1-3. Z component of filtered displacements for PF_90.108.14.25.58, aligned to the arrival times listed in Table 1-1. Pass-band is 0.2 Hz to 1 Hz. Each trace is normalized to the peak value given next to the station name.

Event PF 90.108.14.32.41
For this event, the following problems were found:

	Problem	Resolution
1	Polarity of the following records is reversed: x03y08_n, x01y00_e, x03y15_e.	Polarity of records are corrected
2	Records x03y15_z and x03y15_e (after reversing the polarity) are switched; x03y15_z is actually x03y15_e and x03y15_e is actually x03y15_z.	Mislabeled records are corrected
3	Quality of the following records is questionable: *x03y08_n, x03y15_n.*	Recorded deleted

Figure 1-4 shows the 42 Pinyon Flat Array stations that recorded the 1990 April 18 14:32:41 event. The arrival times of the first P wave on the vertical component are listed in Table 1-2 and plotted in Figure 1-5 for each of the 42 records. The timing error is up to about 0.2 sec.

The displacement records, after aligning the records on the P-wave, are shown in Figure 1-6.

Table 1-2. Arrival Time of P wave from Event PF_90.108.14.32.41

	File Name	Station-East (m)	Station-North (m)	Station-Z	P-wave Arrival Time (sec)
3	x00y00.z	-4.97	15.78	-0.77	9.0123
4	x00y01.z	-5.11	9.21	-2.18	9.0681
5	x00y02.z	-6.42	1.52	-1.83	8.8875
6	x00y04.z	-6.14	-11.59	-2.44	9.0314
7	x00y05.z	-6.7	-18.57	-3.1	8.9815
8	x01y00.z	1.82	15.39	-1.03	9.0123
9	x01y01.z	1.51	9.15	-0.93	9.0696
10	x01y02.z	1.02	2.38	-1.14	8.8890
11	x01y04.z	0.55	-11.67	-2.34	9.0299
12	x01y05.z	0.22	-18.89	-3.27	8.9800
13	x02y00.z	8.24	15.44	0.19	8.9815
14	x02y01.z	9.03	9.49	-0.55	9.1136
15	x02y02.z	7.72	2.08	-1.3	9.0872
16	x02y04.z	7.22	-11.6	-2.34	8.9962
17	x03y00.z	14.96	16.25	-0.34	8.9815
18	x03y01.z	15.1	8.75	-0.97	9.1136
19	x03y02.z	14.7	2.18	-1.44	9.0842
20	x03y04.z	14.5	-11.69	-2.5	8.9932
21	x03y06.z	14.25	-32.35	-4.3	8.9712
22	x03y08.z	10.99	-73.11	-6.52	9.0050
23	x03y09.z	12.13	-93.75	-7.61	9.0299
24	x03y11.z	9.84	-134.8	-10.42	8.9081
25	x03y12.z	9.3	-155.39	-11.38	8.9829
26	x03y13.z	8.14	-176.24	-12.54	8.9095
27	x03y14.z	7.27	-198.16	-14.15	8.9345
28	x03y15.z	7.78	-218.32	-15.85	9.0138
29	x03y16.z	4.87	-239.05	-17.97	8.9389
30	x04y00.z	21.89	16.2	-0.63	8.9595
31	x04y01.z	21.89	8.84	-0.6	9.0211
32	x04y02.z	21.57	2.18	-1.34	8.9903
33	x04y03.z	21.05	-4.61	-1.69	8.8376
34	x05y00.z	29.2	15.69	-0.85	8.9580
35	x05y01.z	28.93	9.31	-0.45	9.0211
36	x05y02.z	28.65	2.17	-1	8.9888
37	x05y03.z	28.55	-4.65	-1.28	8.8376
38	x06y03.z	42.69	-4.65	-1.48	9.0196
39	x11y03.z	146.85	-3.07	-1.34	8.8156
40	x12y03.z	167.69	-2.47	0.07	8.8112
41	x15y03.z	229.52	-2.66	0.41	8.9580
42	x16y03.z	250.13	-4.51	0.96	8.9565

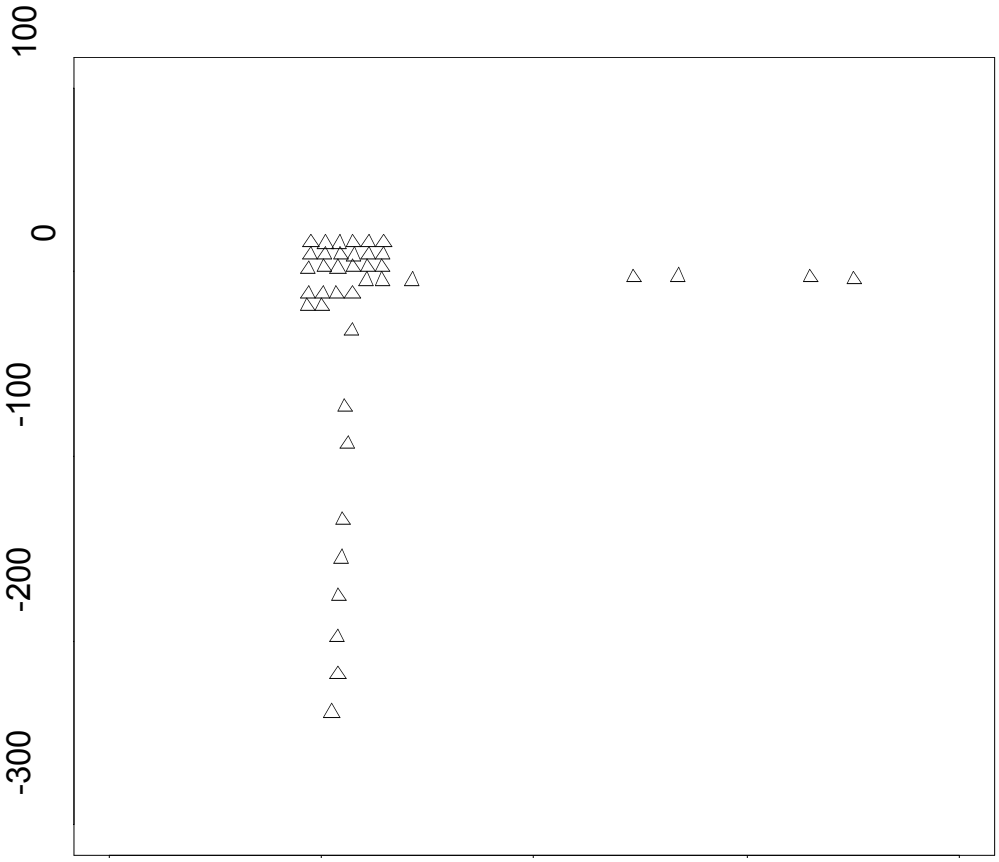

Figure 1-4. Location of stations that recorded event PF_90.108.14.32.41.

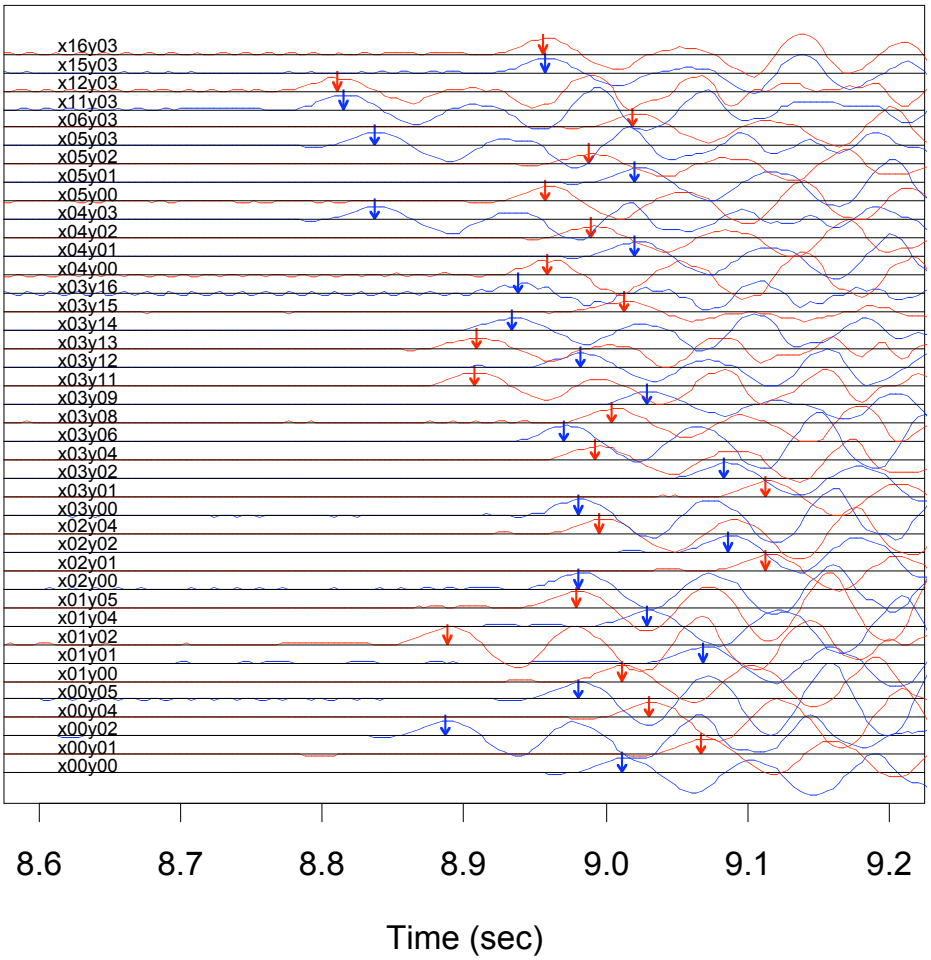

Figure 1-5. Velocity time histories of the Z-component for PF_90.108.14.32.41. The arrows indicate the picked arrival times.

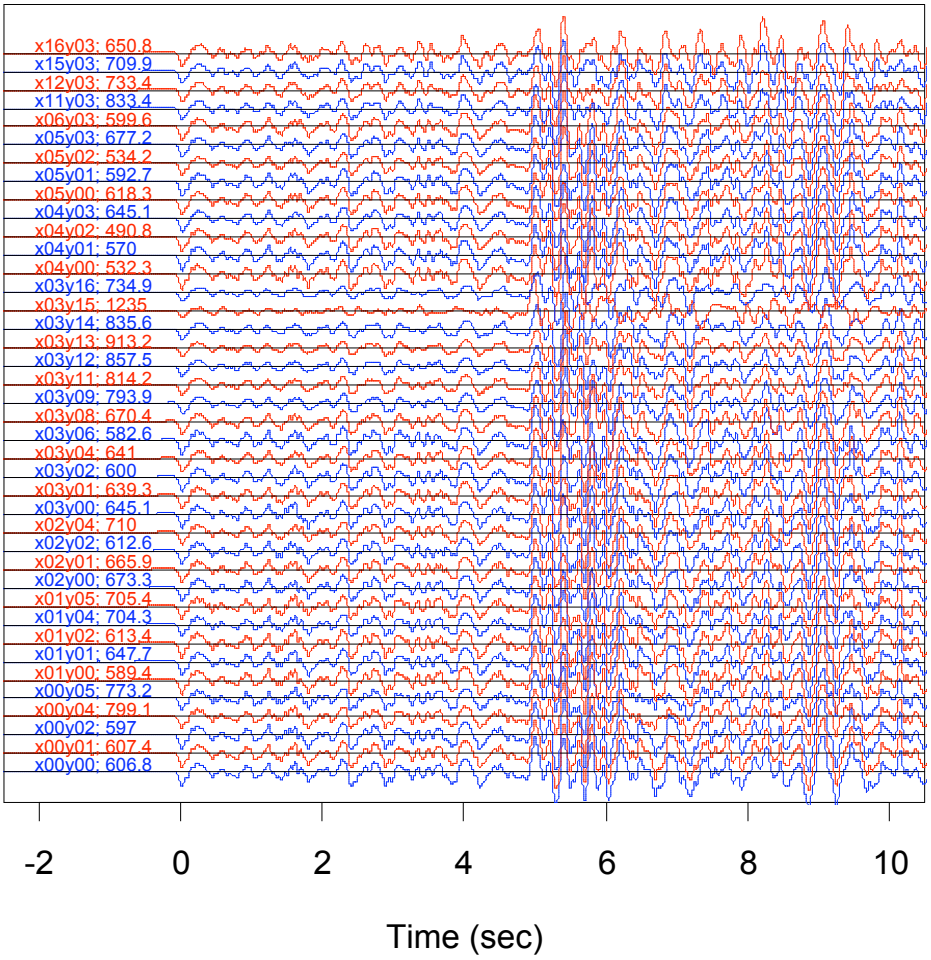

Figure 1-6. Z component of filtered displacements for PF_90.108.14.32.41, aligned to the arrival times listed in Table 1-1. Pass-band is 0.2 Hz to 1 Hz. Each trace is normalized to the peak value given next to the station name.

Event PF 90.122.11.34.56
For this event, the following problems were found:

	Problem	Resolution
1	Polarity of the following records is reversed: x03y08_n.	Polarity is corrected
2	Quality of the following records is questionable: *x03y00_n, x14y03_e, x03y15_e, x03y15_n, x03y15_z.*	Records are excluded
3	Following records are noisy and probably shouldn't be used*: x12y03_n, x03y11_n.*	Records are excluded

Figure 1-7 shows the 56 Pinyon Flat Array stations that recorded the 1990 May 2 11:34:56 event. The arrival times of the first P wave on the vertical component are listed in Table 1-3 and plotted in Figure 1-8 for each of the 56 records. The timing error is up to about 0.2 sec.

The displacement records, after aligning the records on the P-wave, are shown in Figure 1-9.

Table 1-3. Arrival Time of P Wave from Event PF_90.122.11.34.56

	File Name	Station-East (m)	Station-North (m)	Station-Z	P-wave Arrival Time (sec)
3	x00y00_z	-4.97	15.78	-0.77	8.73260
4	x00y01_z	-5.11	9.21	-2.18	8.65073
5	x00y02_z	-6.42	1.52	-1.83	8.70076
6	x00y03_z	-6.4	-4.84	-1.9	8.55369
7	x00y04_z	-6.14	-11.59	-2.44	8.46121
8	x00y05_z	-6.7	-18.57	-3.1	8.54308
9	x01y00_z	1.82	15.39	-1.03	8.73411
10	x01y01_z	1.51	9.15	-0.93	8.65224
11	x01y02_z	1.02	2.38	-1.14	8.70076
12	x01y03_z	0.96	-4.9	-2.09	8.55521
13	x01y04_z	0.55	-11.67	-2.34	8.45818
14	x01y05_z	0.22	-18.89	-3.27	8.54156
15	x02y00_z	8.24	15.44	0.19	8.71440
16	x02y01_z	9.03	9.49	-0.55	8.58856
17	x02y02_z	7.72	2.08	-1.3	8.77808
18	x02y03_z	7.28	-4.6	-1.91	8.49305
19	x02y04_z	7.22	-11.6	-2.34	8.56582
20	x02y05_z	7.1	-18.95	-2.94	8.72047
21	x03y00_z	14.96	16.25	-0.34	8.71592
22	x03y01_z	15.1	8.75	-0.97	8.59008
23	x03y02_z	14.7	2.18	-1.44	8.77657
24	x03y03_z	14.46	-4.8	-2.47	8.64618
25	x03y04_z	14.5	-11.69	-2.5	8.56582
26	x03y05_z	14.43	-18.63	-2.99	8.71895
27	x03y06_z	14.25	-32.35	-4.3	8.62798
28	x03y07_z	13.15	-52.5	-5.64	8.63708
29	x03y08_z	10.99	-73.11	-6.52	8.49608
30	x03y09_z	12.13	-93.75	-7.61	8.73715
31	x03y10_z	9.02	-113.97	-9.23	8.47485
32	x03y11_z	9.84	-134.8	-10.42	8.47789
33	x03y12_z	9.3	-155.39	-11.38	8.60676
34	x03y13_z	8.14	-176.24	-12.54	8.46727
35	x03y15_z	7.78	-218.32	-15.85	8.55218
36	x04y00_z	21.89	16.2	-0.63	8.50214
37	x04y01_z	21.89	8.84	-0.6	8.64315
38	x04y02_z	21.57	2.18	-1.34	8.51882
39	x04y03_z	21.05	-4.61	-1.69	8.68560
40	x04y04_z	21.87	-11.64	-2.12	8.74776
41	x05y00_z	29.2	15.69	-0.85	8.50214
42	x05y01_z	28.93	9.31	-0.45	8.64315
43	x05y02_z	28.65	2.17	-1	8.51731
44	x05y03_z	28.55	-4.65	-1.28	8.68863
45	x05y04_z	28.34	-11.47	-1.98	8.74928
46	x06y03_z	42.69	-4.65	-1.48	8.75382

47	x07y03_z	63.57	-4.67	-1.14	8.68560
48	x08y03_z	84.47	-4.34	-0.88	8.68560
49	x09y03_z	104.86	-2.03	-1.14	8.74473
50	x10y03_z	126.44	-4.55	-0.81	8.74624
51	x11y03_z	146.85	-3.07	-1.34	8.59463
52	x12y03_z	167.69	-2.47	0.07	8.59160
53	x13y03_z	188.77	-2.07	0.19	8.77353
54	x14y03_z	209.66	-2.38	0.56	8.77505
55	x15y03_z	229.52	-2.66	0.41	8.73260
56	x16y03_z	250.13	-4.51	0.96	8.73411

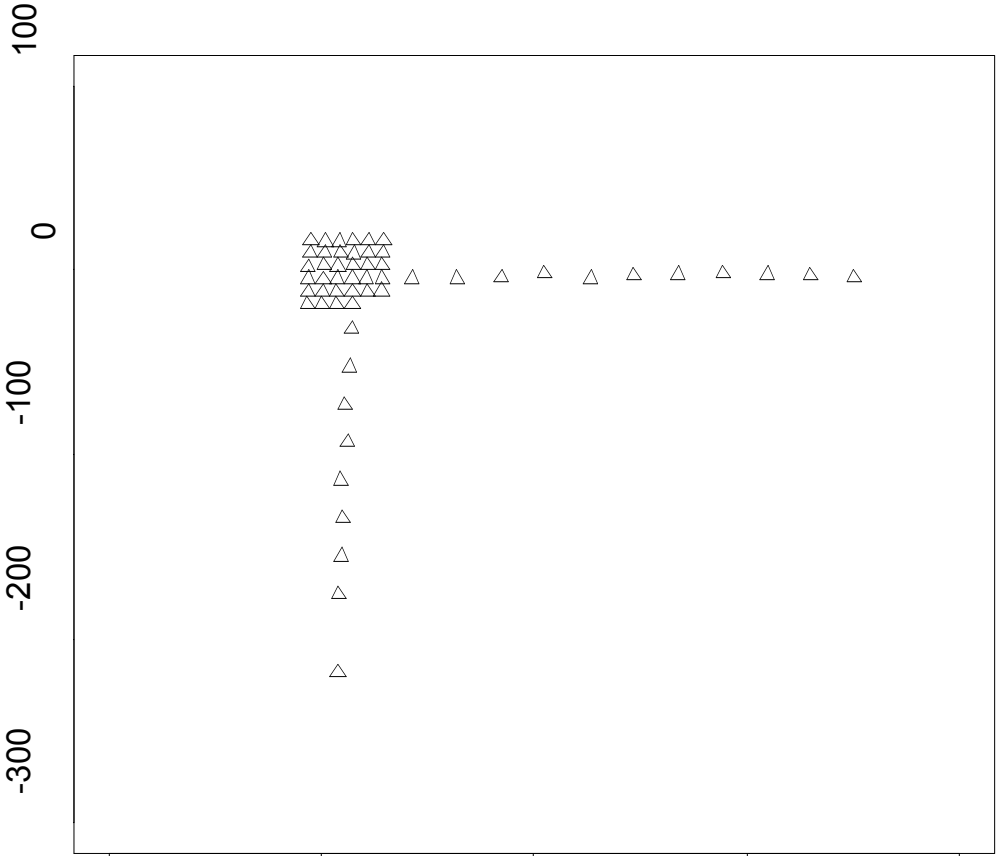

Figure 1-7. Location of stations that recorded event PF_90.122.11.34.56.

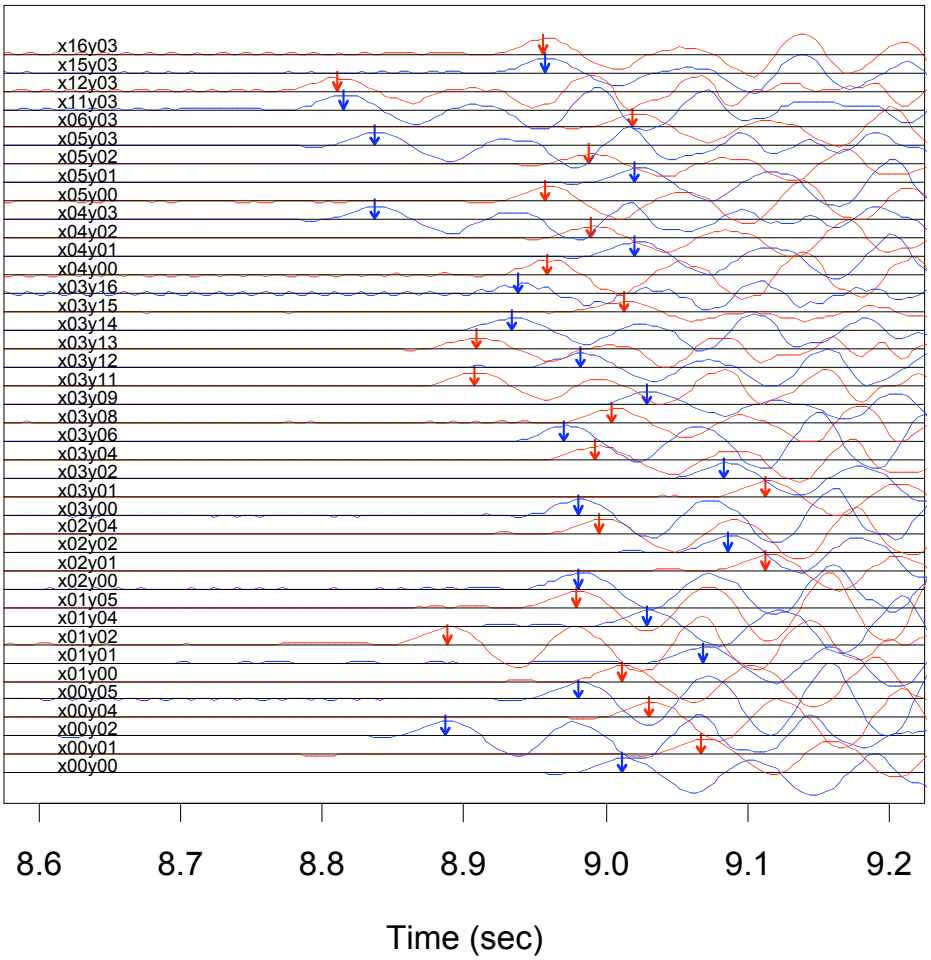

Figure 1-8. Velocity time histories of the Z-component for PF_90.122.11.34.56. The arrows indicate the picked arrival times.

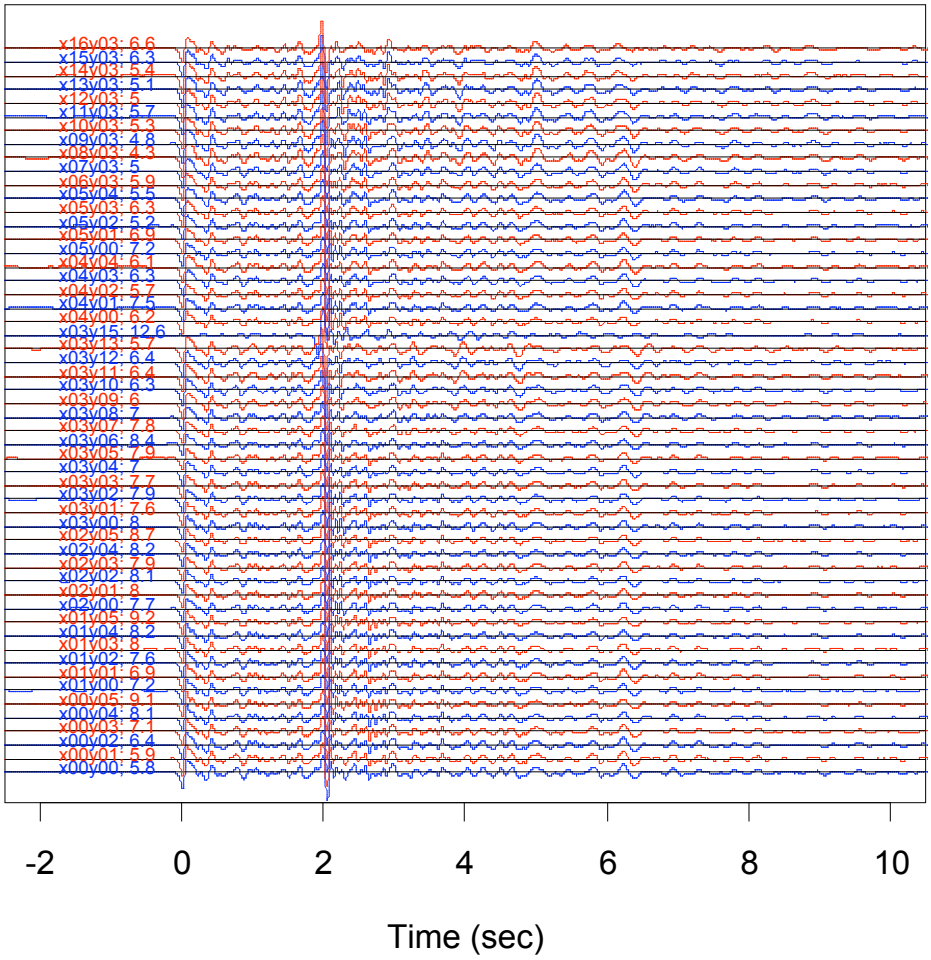

Figure 1-9. Z component of filtered displacements for PF_90.122.11.34.56, aligned to the arrival times listed in Table 1-3. Pass-band is 1 Hz to 5 Hz. Each trace is normalized to the peak value given next to the station name.

Event PF 90.125.08.10.08

For this event, no problems were found for the polarity of the recordings.

Figure 1-10 shows the 48 Pinyon Flat Array stations that recorded the 1990 May 5 08:10:08 event. Arrival time of the first identifiable P wave on the vertical component is listed in Table 1-4 and plotted in Figure 1-11 for each of the 48 records. The timing error is up to about 0.2 sec.

The displacement records, after aligning the records on the P-wave, are shown in Figure 1-12.

Table 1-4. Arrival Time of P Wave from Event PF_90.125.08.10.08

	File Name	Station-East (m)	Station-North (m)	Station-Z	P-wave Arrival Time (sec)
3	x00y01_z	-5.11	9.21	-2.18	8.54355
4	x00y02_z	-6.42	1.52	-1.83	8.54551
5	x00y03_z	-6.4	-4.84	-1.9	8.39577
6	x00y04_z	-6.14	-11.59	-2.44	8.63555
7	x00y05_z	-6.7	-18.57	-3.1	8.38500
8	x01y01_z	1.51	9.15	-0.93	8.54453
9	x01y02_z	1.02	2.38	-1.14	8.54747
10	x01y03_z	0.96	-4.9	-2.09	8.39577
11	x01y04_z	0.55	-11.67	-2.34	8.63359
12	x01y05_z	0.22	-18.89	-3.27	8.38305
13	x02y00_z	8.24	15.44	0.19	8.55725
14	x02y01_z	9.03	9.49	-0.55	8.43100
15	x02y02_z	7.72	2.08	-1.3	8.62283
16	x02y03_z	7.28	-4.6	-1.91	8.67078
17	x02y04_z	7.22	-11.6	-2.34	8.40947
18	x03y00_z	14.96	16.25	-0.34	8.55921
19	x03y01_z	15.1	8.75	-0.97	8.43198
20	x03y02_z	14.7	2.18	-1.44	8.62185
21	x03y03_z	14.46	-4.8	-2.47	8.48679
22	x03y04_z	14.5	-11.69	-2.5	8.40849
23	x03y06_z	14.25	-32.35	-4.3	8.52887
24	x03y07_z	13.15	-52.5	-5.64	8.47994
25	x03y08_z	10.99	-73.11	-6.52	8.35466
26	x03y09_z	12.13	-93.75	-7.61	8.57976
27	x03y10_z	9.02	-113.97	-9.23	8.65219
28	x03y11_z	9.84	-134.8	-10.42	8.39773
29	x03y12_z	9.3	-155.39	-11.38	8.50832
30	x03y13_z	8.14	-176.24	-12.54	8.38794
31	x03y15_z	7.78	-218.32	-15.85	8.33411
32	x04y01_z	21.89	8.84	-0.6	8.66883
33	x04y03_z	21.05	-4.61	-1.69	8.49658
34	x04y04_z	21.87	-11.64	-2.12	8.59151
35	x04y05_z	21.57	-18.51	-2.78	8.66883
36	x05y01_z	28.93	9.31	-0.45	8.66883
37	x05y03_z	28.55	-4.65	-1.28	8.49853
38	x05y04_z	28.34	-11.47	-1.98	8.59347
39	x05y05_z	28.48	-19.04	-2.65	8.66785
40	x06y03_z	42.69	-4.65	-1.48	8.59542
41	x07y03_z	63.57	-4.67	-1.14	8.36445
42	x08y03_z	84.47	-4.34	-0.88	8.36445
43	x09y03_z	104.86	-2.03	-1.14	8.58759
44	x10y03_z	126.44	-4.55	-0.81	8.58955
45	x11y03_z	146.85	-3.07	-1.34	8.43590
46	x12y03_z	167.69	-2.47	0.07	8.43590

47	x15y03_z	229.52	-2.66	0.41	8.54845
48	x16y03_z	250.13	-4.51	0.96	8.54845

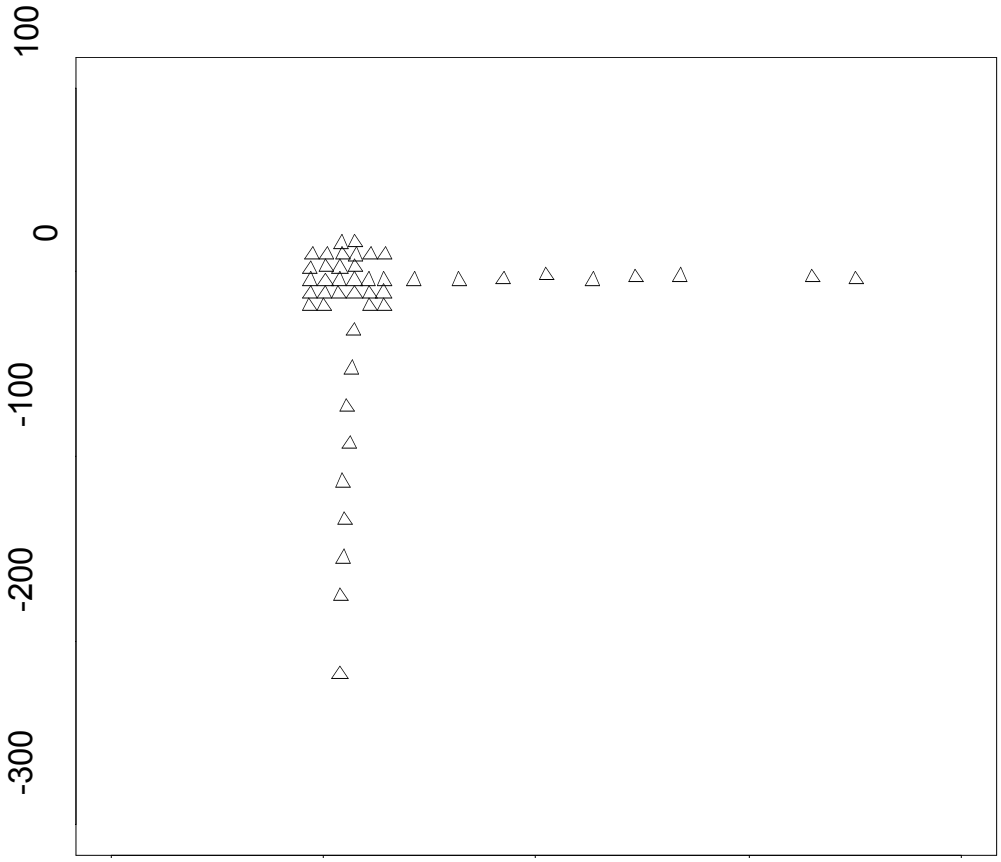

Figure 1-10. Location of stations that recorded event PF_90.125.08.10.08.

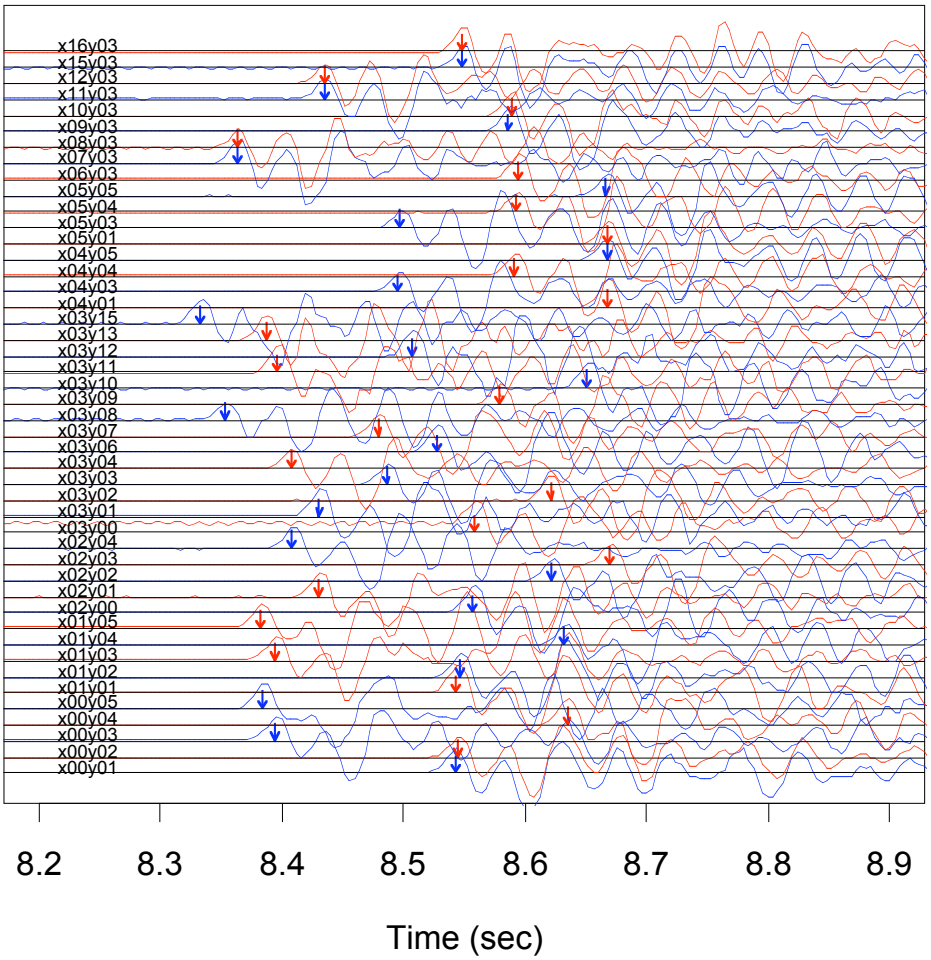

Figure 1-11. Acceleration time histories of the Z components near the first P arrivals for PF_90.125.08.10.08. The arrows indicate the picked arrival times.

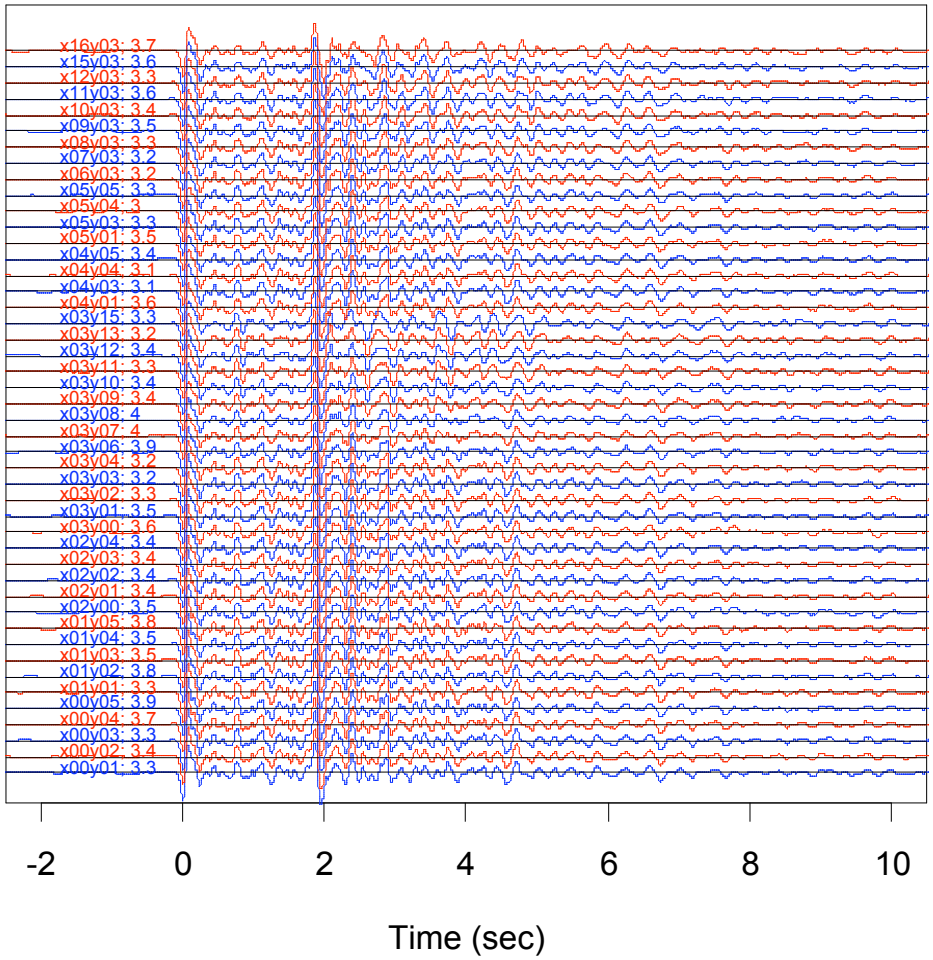

Figure 1-12. Z component of filtered displacements for PF_90.125.08.10.08, aligned to the arrival times listed in Table 1-4. Pass-band is 1 Hz to 5 Hz. Each trace is normalized to the peak value given next to the station name.

Event PF 90.134.05.05.20
For this event, the following problems were found:

	Problem	Resolution
1	**The data quality of *x03y11_n* is poor.**	Record x03y11_n is excluded

Figure 1-13 shows the 60 Pinyon Flat Array stations that recorded the 1990 May 14 05:05:20 event. Arrival time of the first identifiable P wave on the vertical component is listed in Table 1-5 and plotted in Figure 1-14 for each of the 60 records. The timing error is up to about 0.2 sec.

The displacement records, after aligning the records on the P-wave, are shown in Figure 1-15.

Table 1-5. Arrival Time of P Wave from Event PF_90.134.05.05.20

	File Name	Station-East (m)	Station-North (m)	Station-Z	P-wave Arrival Time (sec)
3	x00y00_z	-4.97	15.78	-0.77	8.90241
4	x00y01_z	-5.11	9.21	-2.18	8.88096
5	x00y02_z	-6.42	1.52	-1.83	8.59410
6	x00y03_z	-6.4	-4.84	-1.9	8.77818
7	x00y04_z	-6.14	-11.59	-2.44	8.67654
8	x00y05_z	-6.7	-18.57	-3.1	8.63927
9	x01y00_z	1.82	15.39	-1.03	8.90467
10	x01y01_z	1.51	9.15	-0.93	8.88434
11	x01y02_z	1.02	2.38	-1.14	8.59748
12	x01y03_z	0.96	-4.9	-2.09	8.77818
13	x01y04_z	0.55	-11.67	-2.34	8.67654
14	x01y05_z	0.22	-18.89	-3.27	8.63927
15	x02y00_z	8.24	15.44	0.19	8.62120
16	x02y01_z	9.03	9.49	-0.55	8.81997
17	x02y02_z	7.72	2.08	-1.3	8.65282
18	x02y03_z	7.28	-4.6	-1.91	8.72736
19	x02y04_z	7.22	-11.6	-2.34	8.79400
20	x02y05_z	7.1	-18.95	-2.94	8.78270
21	x03y00_z	14.96	16.25	-0.34	8.62120
22	x03y01_z	15.1	8.75	-0.97	8.81658
23	x03y02_z	14.7	2.18	-1.44	8.65282
24	x03y03_z	14.46	-4.8	-2.47	8.87305
25	x03y04_z	14.5	-11.69	-2.5	8.79400
26	x03y05_z	14.43	-18.63	-2.99	8.78270
27	x03y06_z	14.25	-32.35	-4.3	8.64266
28	x03y07_z	13.15	-52.5	-5.64	8.86740
29	x03y08_z	10.99	-73.11	-6.52	8.78157
30	x03y09_z	12.13	-93.75	-7.61	8.56586
31	x03y10_z	9.02	-113.97	-9.23	8.71494
32	x03y11_z	9.84	-134.8	-10.42	8.74430
33	x03y12_z	9.3	-155.39	-11.38	8.62798
34	x03y13_z	8.14	-176.24	-12.54	8.73753
35	x03y14_z	7.27	-198.16	-14.15	8.66186
36	x03y15_z	7.78	-218.32	-15.85	8.77028
37	x03y16_z	4.87	-239.05	-17.97	8.65847
38	x04y00_z	21.89	16.2	-0.63	8.69461
39	x04y01_z	21.89	8.84	-0.6	8.72172
40	x04y02_z	21.57	2.18	-1.34	8.87079
41	x04y03_z	21.05	-4.61	-1.69	8.85046
42	x04y04_z	21.87	-11.64	-2.12	8.80868
43	x04y05_z	21.57	-18.51	-2.78	8.72849
44	x05y00_z	29.2	15.69	-0.85	8.69461
45	x05y01_z	28.93	9.31	-0.45	8.72172
46	x05y02_z	28.65	2.17	-1	8.86966

47	x05y03_z	28.55	-4.65	-1.28	8.85159
48	x05y04_z	28.34	-11.47	-1.98	8.80981
49	x05y05_z	28.48	-19.04	-2.65	8.72849
50	x06y03_z	42.69	-4.65	-1.48	8.57941
51	x07y03_z	63.57	-4.67	-1.14	8.90806
52	x08y03_z	84.47	-4.34	-0.88	8.91032
53	x09y03_z	104.86	-2.03	-1.14	8.78383
54	x10y03_z	126.44	-4.55	-0.81	8.78835
55	x11y03_z	146.85	-3.07	-1.34	8.84143
56	x12y03_z	167.69	-2.47	0.07	8.84256
57	x13y03_z	188.77	-2.07	0.19	8.60539
58	x14y03_z	209.66	-2.38	0.56	8.60878
59	x15y03_z	229.52	-2.66	0.41	8.85498
60	x16y03_z	250.13	-4.51	0.96	8.88083

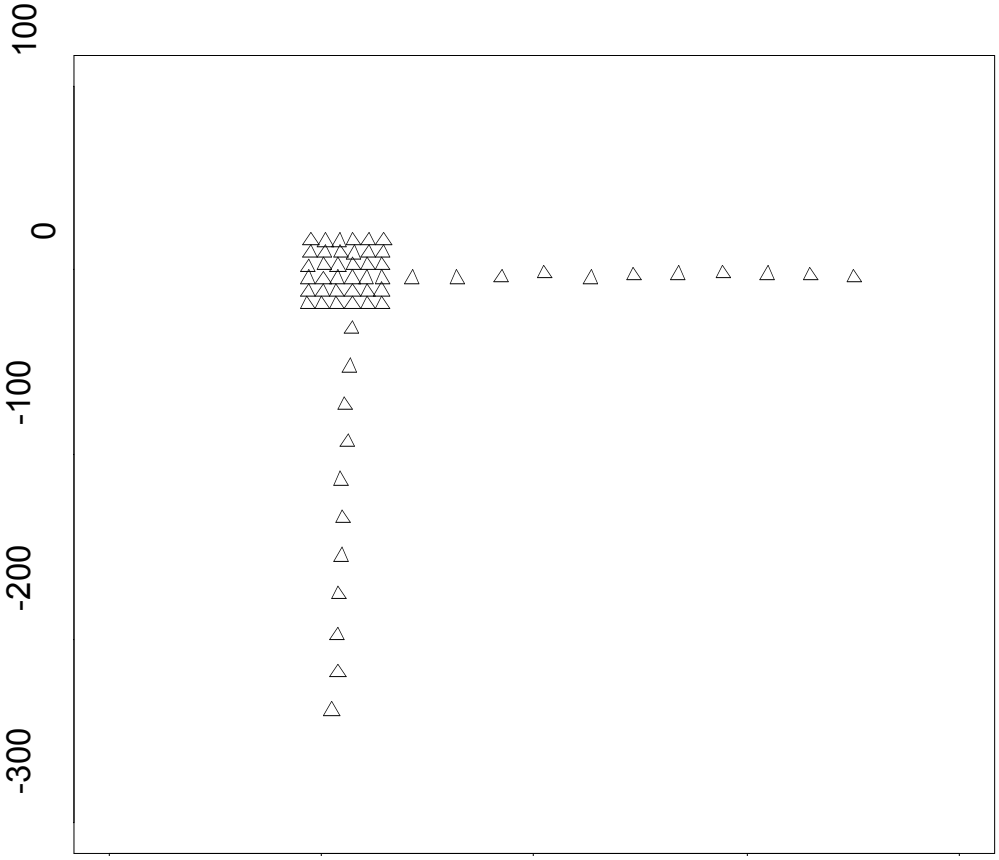

Figure 1-13. Location of stations that recorded event PF_90.134.05.05.20.

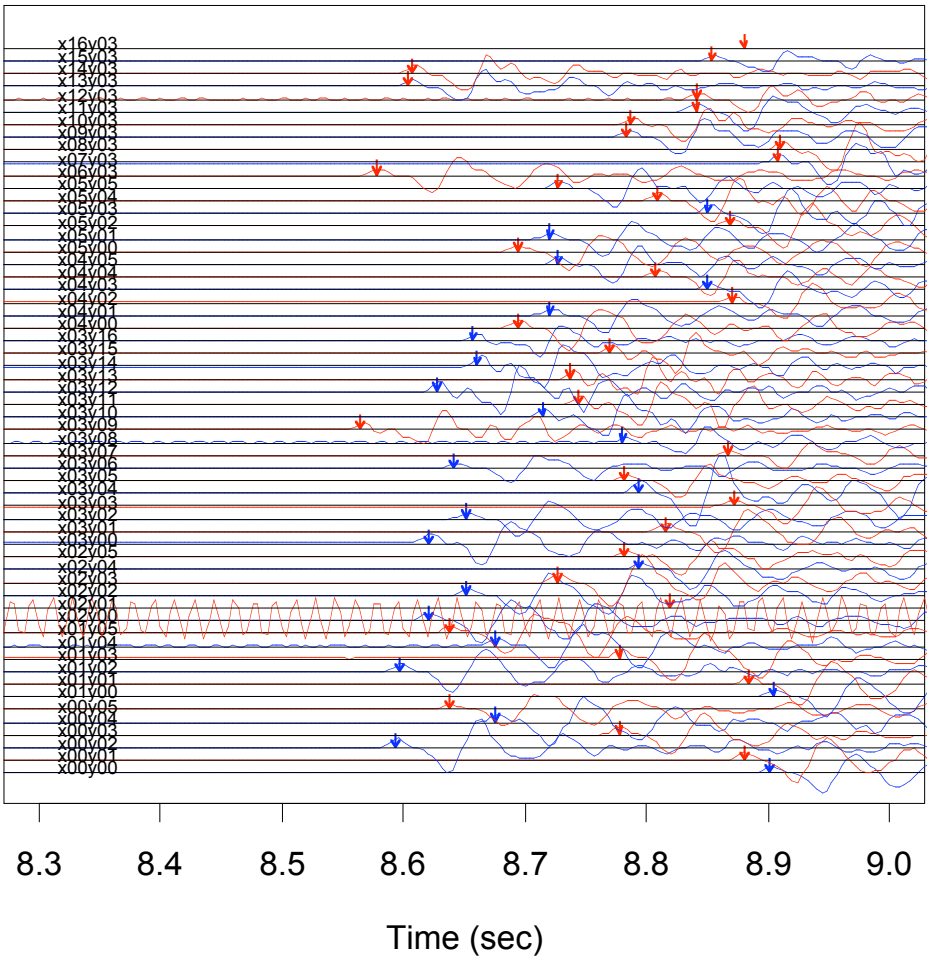

Figure 1-14. Velocity time histories of the Z components near the first P arrivals for PF_90.134.05.05.20. The arrows indicate the arrival times picked.

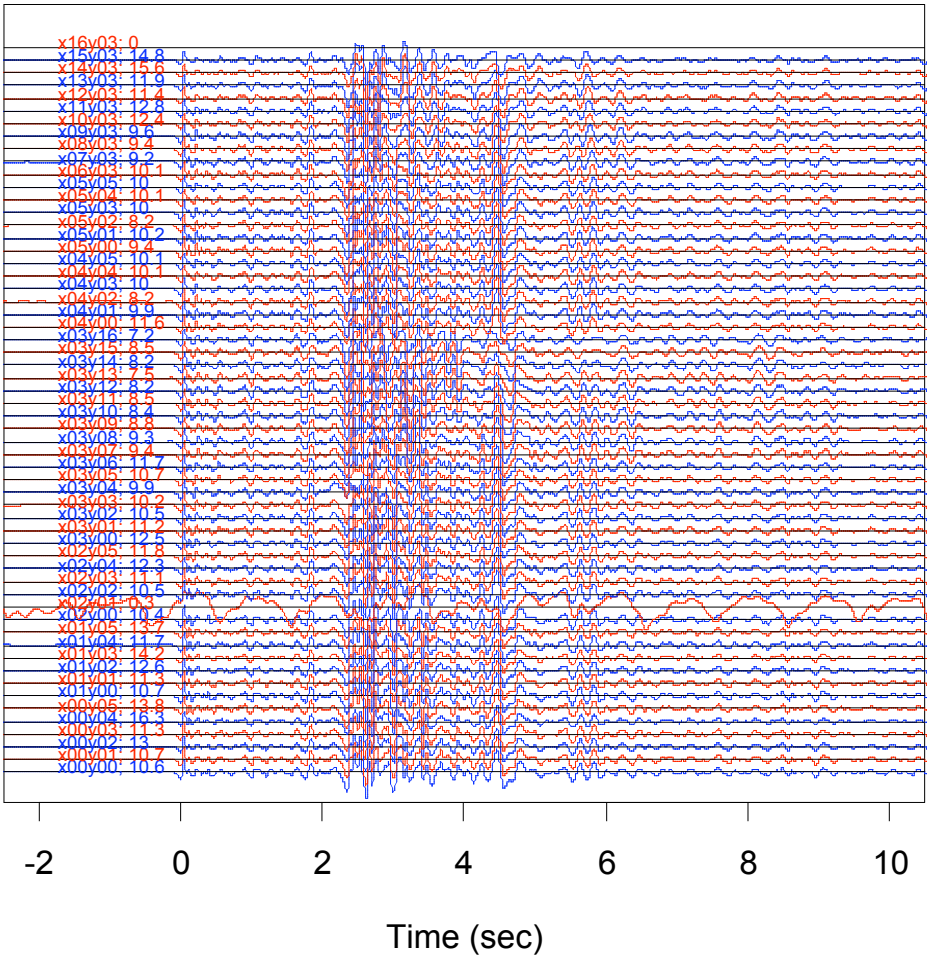

Figure 1-15. Z component of filtered displacements for PF_90.134.05.05.20, aligned to the arrival times listed in Table 1-5. Pass-band is 1 Hz to 5 Hz. Each trace is normalized to the peak value given next to the station name.

Event PF 90.136.01.14.15

For this event, the following problems were found:

	Problem	Resolution
1	**The wavefield of N component is more complicated than the wavefields of the other two components. The primary S waves on N component seem to consist of multiple waves propagating at different direction. This, along with the short duration, makes the identification of polarity reversal on N component difficult.**	NS components are included.
2	**Several records (*x03y00_n*, *x03y05_n*, *x03y07_n*, and *x03y16_n*) may have polarity problem based on the waveform of primary S wave. However, the coda on these records just before the 5 sec time mark suggests otherwise.**	No polarity change is made

Figure 1-16 shows the 55 Pinyon Flat Array stations that recorded the 1990 May 16 01:14:15 event. Arrival time of the first identifiable P wave on the vertical component is listed in Table 1-6 and plotted in Figure 1-17 for each of the 55 records.

Table 1-6. Arrival Time of P Wave from Event PF_90.136.01.14.15

	File Name	Station-East (m)	Station-North (m)	Station-Z	P-wave Arrival Time (sec)
1	x00y00_z	-4.97	15.78	-0.77	8.79516
2	x00y01_z	-5.11	9.21	-2.18	8.81824
3	x00y02_z	-6.42	1.52	-1.83	8.62308
4	x00y03_z	-6.4	-4.84	-1.9	8.67019
5	x00y04_z	-6.14	-11.59	-2.44	8.89995
6	x00y05_z	-6.7	-18.57	-3.1	8.86246
7	x01y00_z	1.82	15.39	-1.03	8.79709
8	x01y01_z	1.51	9.15	-0.93	8.82016
9	x01y02_z	1.02	2.38	-1.14	8.62308
10	x01y03_z	0.96	-4.9	-2.09	8.66827
11	x01y04_z	0.55	-11.67	-2.34	8.89803
12	x01y05_z	0.22	-18.89	-3.27	8.85957
13	x02y00_z	8.24	15.44	0.19	8.84227
14	x02y02_z	7.72	2.08	-1.3	8.87303
15	x02y03_z	7.28	-4.6	-1.91	8.61539
16	x02y04_z	7.22	-11.6	-2.34	8.60674
17	x02y05_z	7.1	-18.95	-2.94	8.67019
18	x03y00_z	14.96	16.25	-0.34	8.84323
19	x03y01_z	15.1	8.75	-0.97	8.70384
20	x03y02_z	14.7	2.18	-1.44	8.87111
21	x03y03_z	14.46	-4.8	-2.47	8.75863
22	x03y04_z	14.5	-11.69	-2.5	8.60578
23	x03y05_z	14.43	-18.63	-2.99	8.66923
24	x03y06_z	14.25	-32.35	-4.3	8.61347
25	x03y07_z	13.15	-52.5	-5.64	8.75190
26	x03y08_z	10.99	-73.11	-6.52	8.57309
27	x03y09_z	12.13	-93.75	-7.61	8.77978
28	x03y10_z	9.02	-113.97	-9.23	8.59713
29	x03y12_z	9.3	-155.39	-11.38	8.59040
30	x03y13_z	8.14	-176.24	-12.54	8.70384
31	x03y14_z	7.27	-198.16	-14.15	8.55290
32	x03y15_z	7.78	-218.32	-15.85	8.55290
33	x03y16_z	4.87	-239.05	-17.97	8.54618
34	x04y00_z	21.89	16.2	-0.63	8.68076
35	x04y01_z	21.89	8.84	-0.6	8.60770
36	x04y02_z	21.57	2.18	-1.34	8.75479
37	x04y03_z	21.05	-4.61	-1.69	8.81727
38	x04y04_z	21.87	-11.64	-2.12	8.69422
39	x04y05_z	21.57	-18.51	-2.78	8.86919
40	x05y00_z	29.2	15.69	-0.85	8.68076
41	x05y01_z	28.93	9.31	-0.45	8.60770
42	x05y02_z	28.65	2.17	-1	8.75479
43	x05y03_z	28.55	-4.65	-1.28	8.81920
44	x05y04_z	28.34	-11.47	-1.98	8.69614

45	x05y05_z	28.48	-19.04	-2.65	8.86919
46	x06y03_z	42.69	-4.65	-1.48	8.79516
47	x07y03_z	63.57	-4.67	-1.14	8.79036
48	x08y03_z	84.47	-4.34	-0.88	8.78747
49	x09y03_z	104.86	-2.03	-1.14	8.65961
50	x10y03_z	126.44	-4.55	-0.81	8.66058
51	x11y03_z	146.85	-3.07	-1.34	8.70960
52	x12y03_z	167.69	-2.47	0.07	8.70768
53	x13y03_z	188.77	-2.07	0.19	8.61539
54	x15y03_z	229.52	-2.66	0.41	8.70960
55	x16y03_z	250.13	-4.51	0.96	8.70864

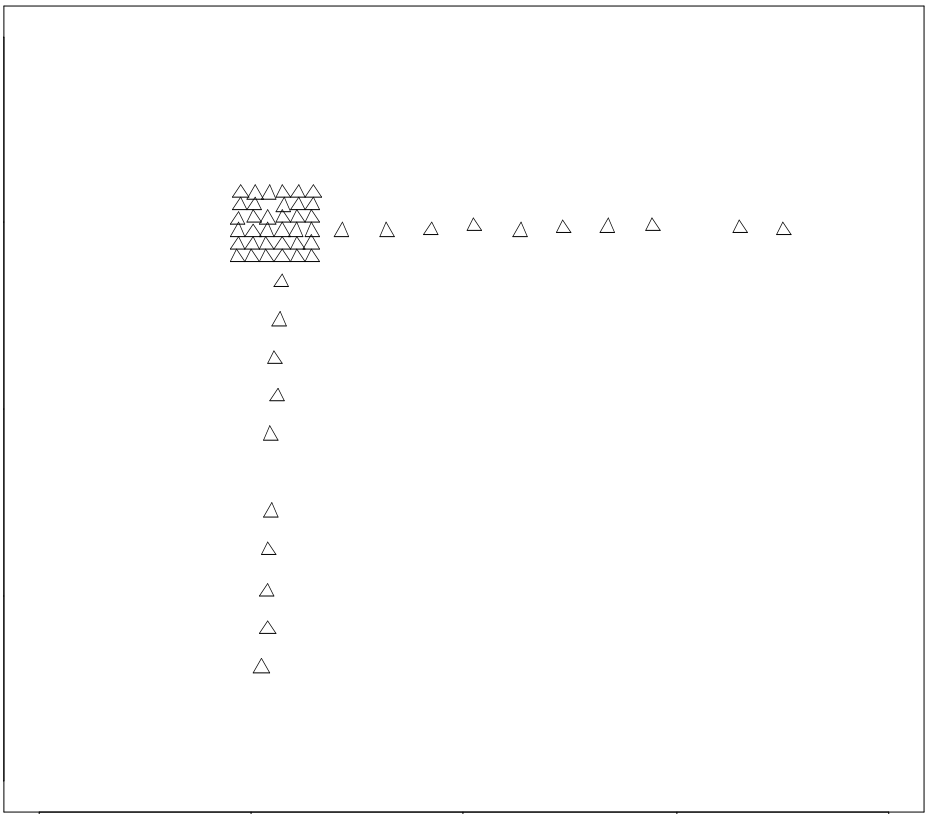

Figure 1-17. Location of stations that recorded event PF_90.136.01.14.15.

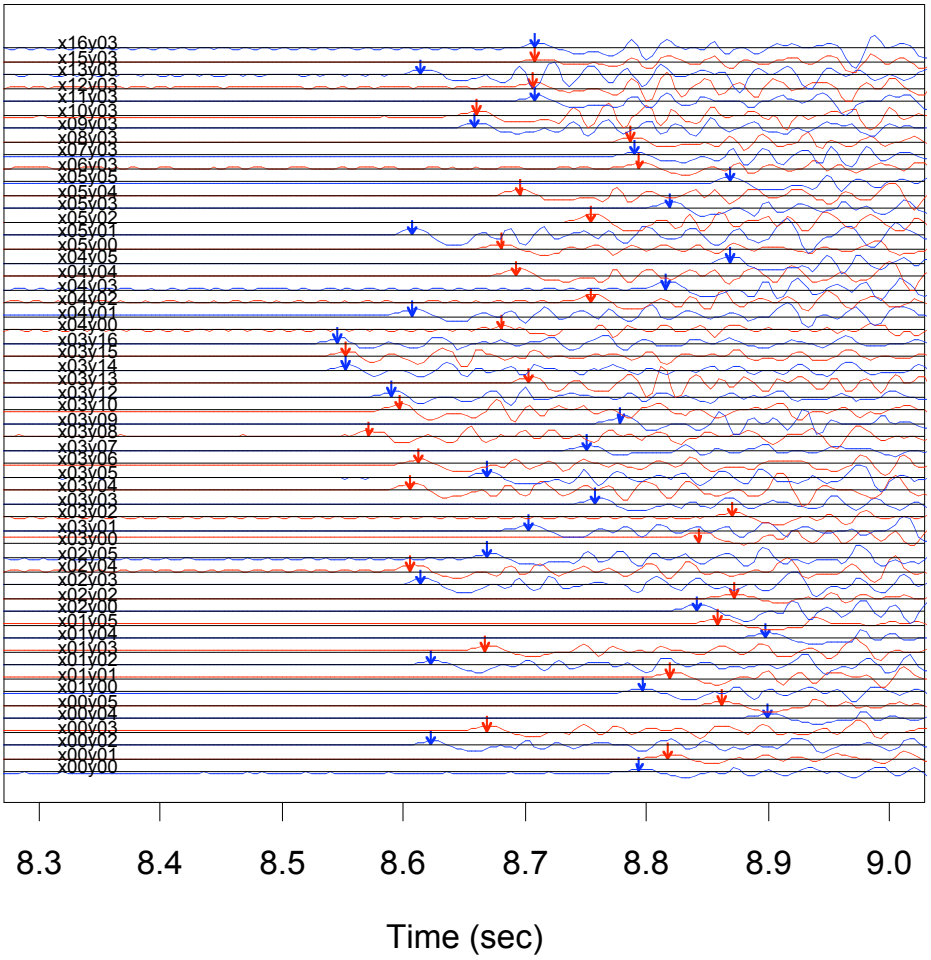

Figure 1-18. Acceleration time histories of the Z component near the first P arrivals for PF_90.136.01.14.15. The arrows indicate the arrival times picked.

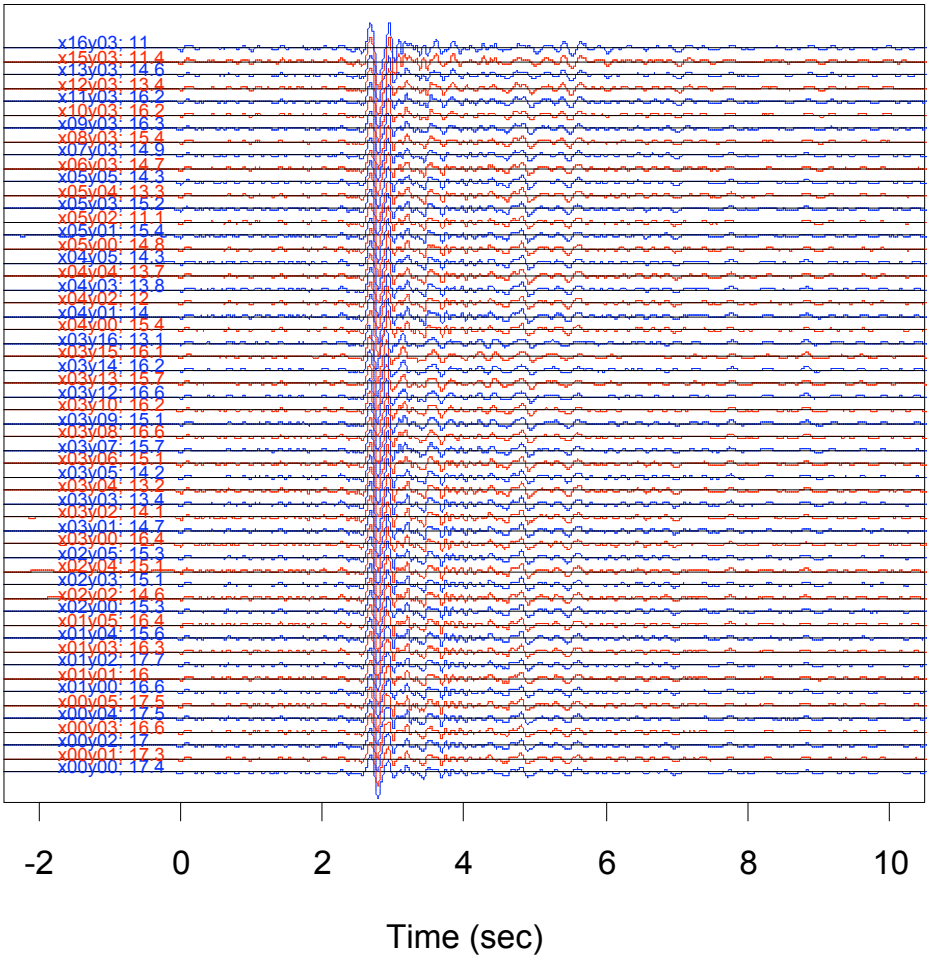

Figure 1-18. Z component of filtered displacements for PF_90.136.01.14.15, aligned to the arrival times listed in Table 1-6. Pass-band is 1 Hz to 5 Hz. Each trace is normalized to the peak value given next to the station name.

Plane-Wave Residuals for PF data

The Pinyon Flat data aligned on the P-wave arrival were used to compare with the plane-wave coherency model. The residuals are shown in Figures 1-19. There is a positive average residual (under-prediction) of the short separation (0-60m) and high frequency (10-40 Hz) plane-wave coherency for the aligned data. This under-prediction is greater than the under-prediction found for the coherency at depth (Item 2 below). At separation distances of 60-150m, the model works well and the residuals are small.

Since the recordings were aligned on the P-wave arrival, there may be a bias toward increased plane-wave coherency since any randomness in the arrival times has been removed. This would affect the coherency at high frequencies ($f > 15$ Hz). The apparent velocity of the P-waves is typically about 5 km/s. For a station separation of 25 m, this corresponds to a delay time of 0.005 sec. From other dense arrays with correct timing, we have seen there is variability in the measured slowness over distances of tens of meters comparable to the expected delay time. If we consider that there could be variations of about 0.005 sec in the arrival times across separation distances of 10-60 m, then this would correspond to 1/10 of a cycle for 20 Hz which would significantly reduce the coherency.

As an example, the coherency residuals are compared for the aligned PF data (PF_90.136.01.14.15) and the aligned data with a small variability (normally distributed variability in the lag times with a standard deviation of 0.005 sec). The result of this small variability is to reduce the residuals at high frequencies to be about 0.1 units (Figure 1-20). This is comparable to the correction needed for embedment (see Item 2). This would suggest that for hard rock sites, the surface coherency is similar to the coherency at depths of 10-20 m for soil sites (see Figures 2-1 and 2-2)

The soft-rock data do not show the same trend of increased coherency as compared to the model. The plane-wave coherency residuals for the soft-rock and soil sites are shown in Figures 1-21 and 1-22, respectively.

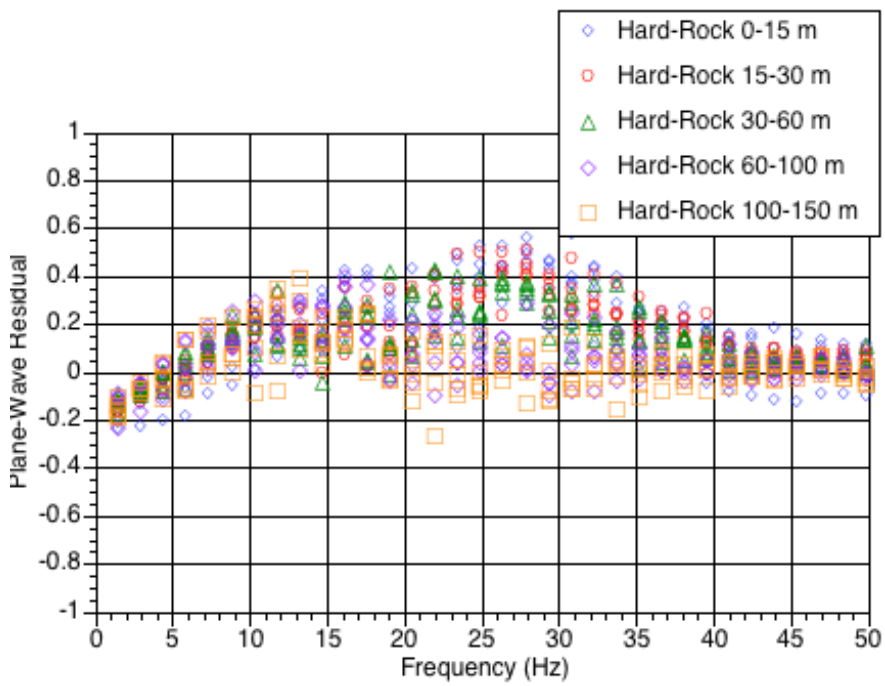

Figure 1-19. Plane-wave coherency residual for the Pinyon Flat data aligned on the P-wave arrival.

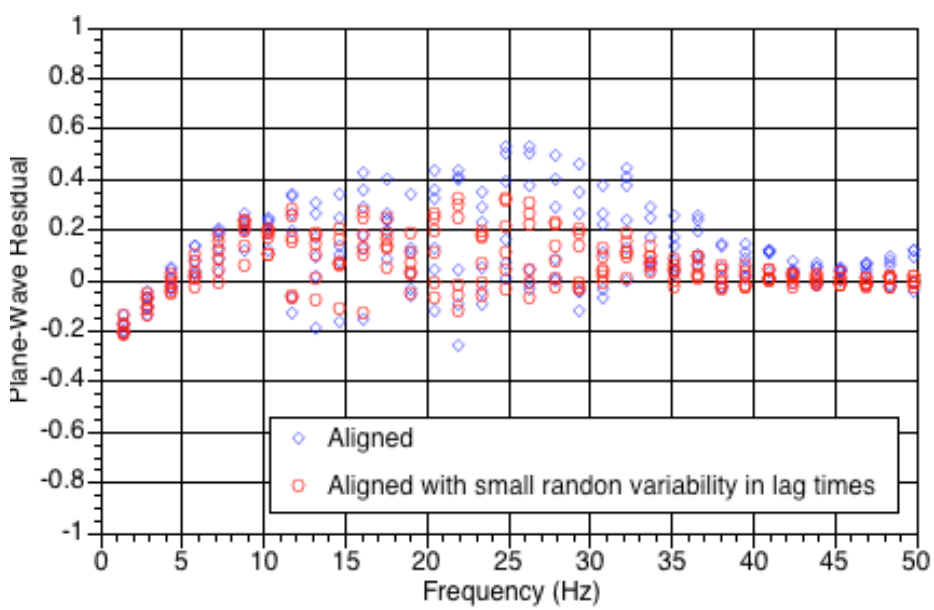

Figure 1-20. Example of the effect of a small amount of variability (0.005 sec) in the P-wave arrival time on the plane-wave coherency residual.

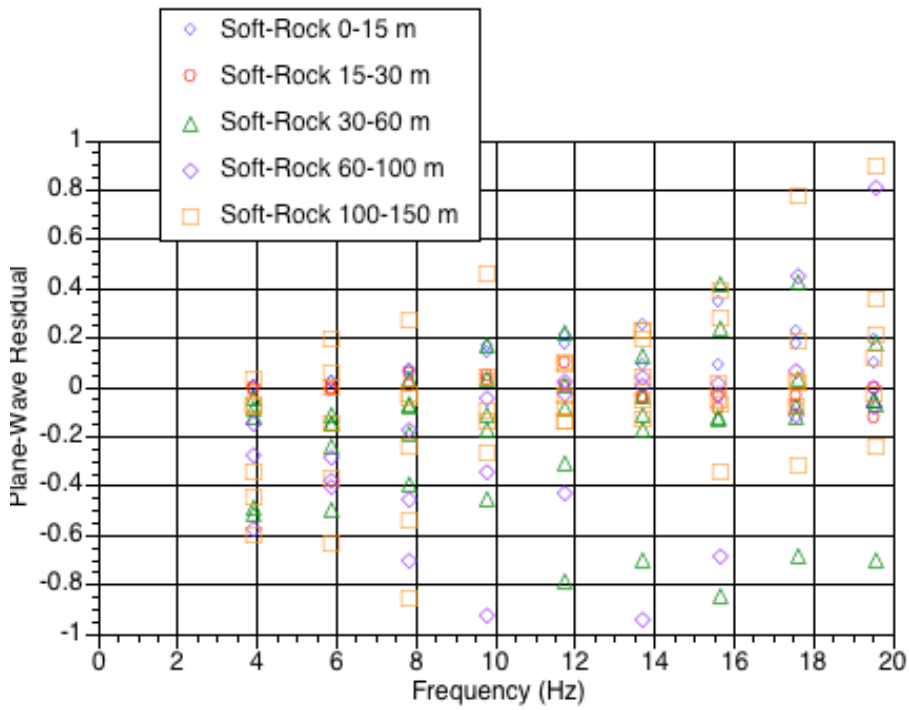

Figure 1-21. Plane-wave residuals for soft-rock sites.

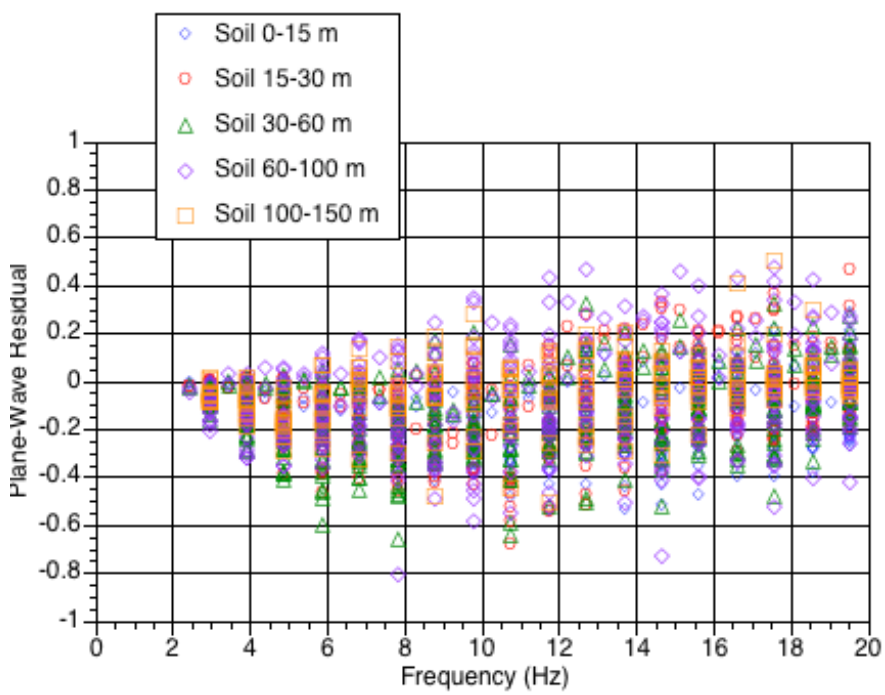

Figure 1-21. Plane-wave residuals for soil sites.

Item 2. Develop a new coherency model for embedded structures

The response to RAI Q5.4 evaluated the residuals of the plane-wave coherency from stations at depths of 10-20 m (see Appendix A). The limited coherency at depths of embedment indicated that the proposed plane-wave coherency model underestimated the coherency by about 0.1 units over the frequency band of 10-20 Hz (Figure 2-1). To account for this difference, a revised coherency model was developed for embedment depths of 10-20m.

The plane-wave coherency model is given by

$$\gamma_{pw}(f,\xi) = \left[1 + \left(\frac{f\,Tanh(a_3\xi)}{a_1 f_c(\xi)}\right)^{n1}\right]^{-1/2} \left[1 + \left(\frac{f\,Tanh(a_3\xi)}{a_2 f_c(\xi)}\right)^{n2(\xi)}\right]^{-1/2}$$

For the coherency for embedment depth of 10-20m, the following form is used:

$$\gamma_{pw,Embed}(f,\xi) = \left[1 + \left(\frac{f\,Tanh(a_3\xi)}{b_1 f_c(\xi)}\right)^{n1}\right]^{-1/2} \left[1 + \left(\frac{f\,Tanh(a_3\xi)}{b_2 f_c(\xi)}\right)^{n2(\xi)}\right]^{-1/2}$$

where

$b_1 = 1.15\ a_1$
$b_2 = 1.15\ a_2$

All other coefficients are unchanged. The revised model is compared to the surface coherency model in Figure 2-2.

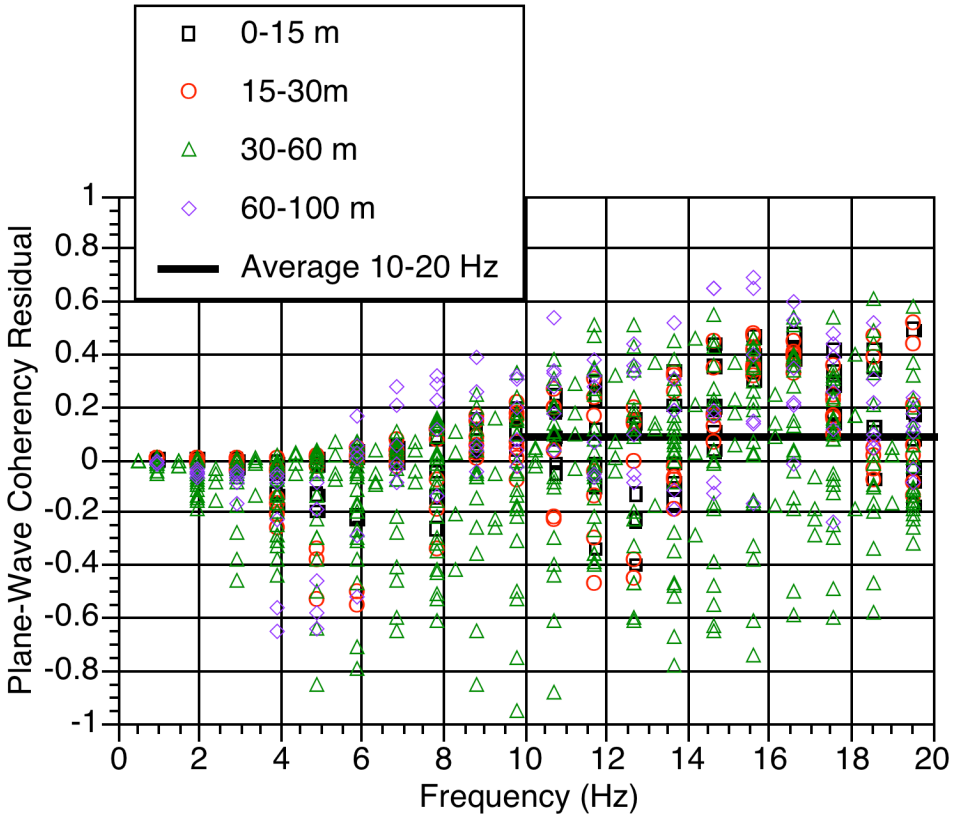

Figure 2-1. Residuals of the plane-wave coherency from stations at depths of 10-20m based on the surface coherency model. (From appendix A, response to RAI Q5.4)

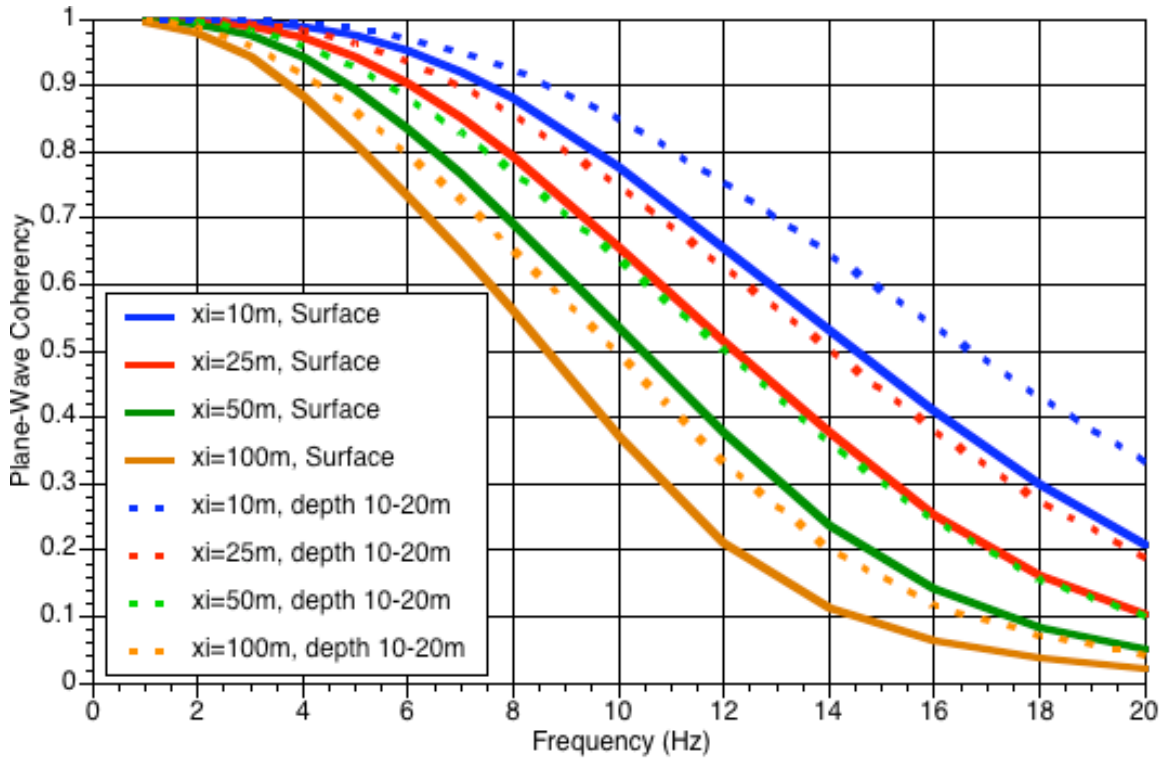

Figure 2-2. Comparison of the horizontal component coherency models for the surface and embedment depths of 10-20 m.

Item 3. Correlation of FAS and Coherency

At the Oct 24, 2006 coherency meeting, one item discussed was the possible correlation of the FAS and the coherency. The suggestion was that the high frequency coherency may be higher when there is greater power in the high frequencies. Such a correlation would be important for the application to the EUS since the EUS rock spectra are peaked at higher frequencies than most of the data used to develop the empirical coherency model.

To test this correlation, the average FAS for each earthquake was computed and a then normalized by the peak amplitude. The average was computed using the geometric mean. The plane-wave coherency residuals are plotted against the normalized spectral amplitude. The analysis is conducted separately for the aligned Pinyon Flat data since this data was seen to has a large overall positive residual.

The residuals for the data set excluding Pinyon Flat are shown in Figures 3-1 and 3-2 for frequency bands of 13-17 Hz and 18-20 Hz, respectively. The residuals do not show a positive trend with the normalized spectral value.

The residuals for the Pinyon Flat data are shown in Figures 3-3 and 3-4 for frequency bands of 13-17 Hz and 25-30 Hz, respectively. While these data show an overall shift to positive residuals, there is no trend with the normalized spectral value.

We conclude that FAS is not correlated with the location of the peak in the spectrum.

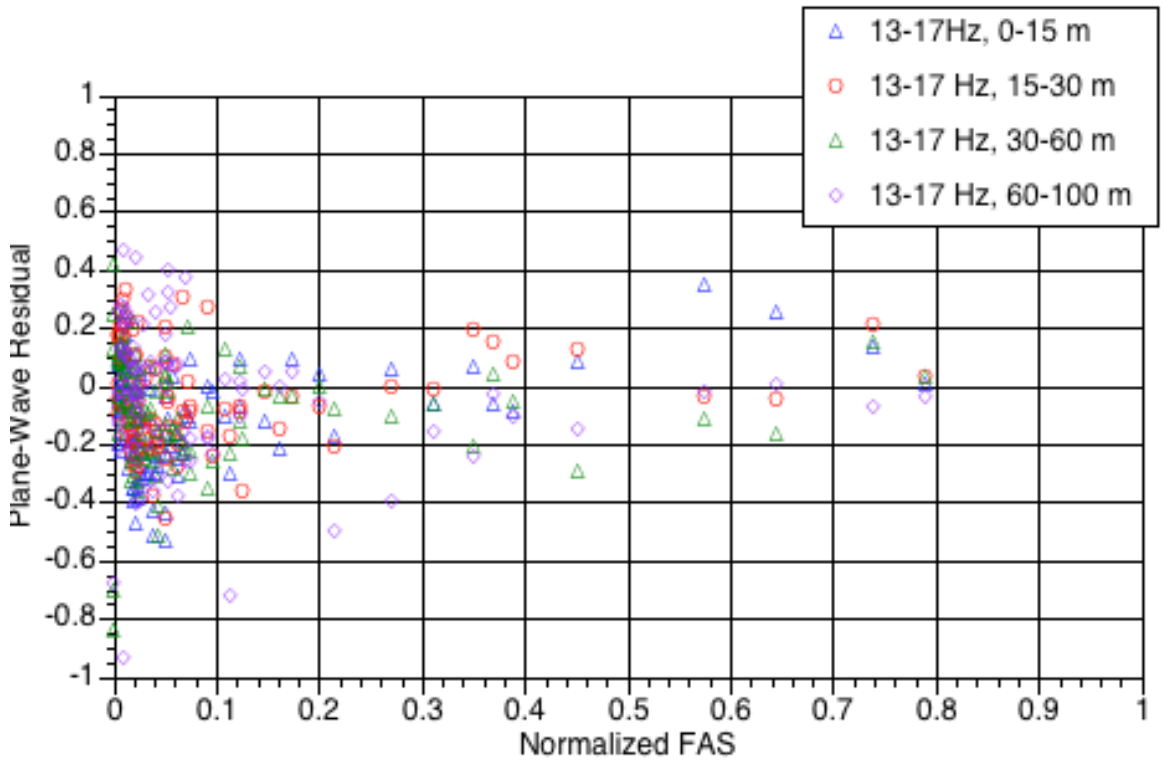

Figure 3-1. Plane-Wave coherency residuals for 13-17 Hz, excluding the Pinyon Flat data

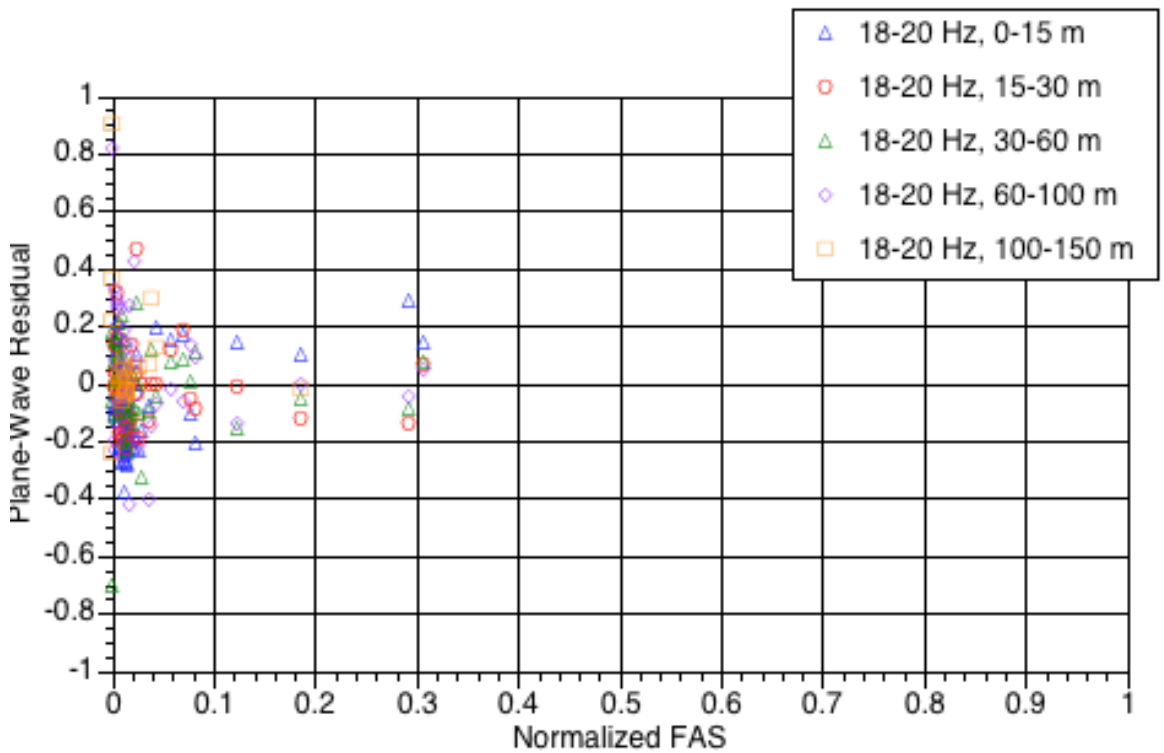

Figure 3-2. Plane-Wave coherency residuals for 18-20 Hz, excluding the Pinyon Flat data.

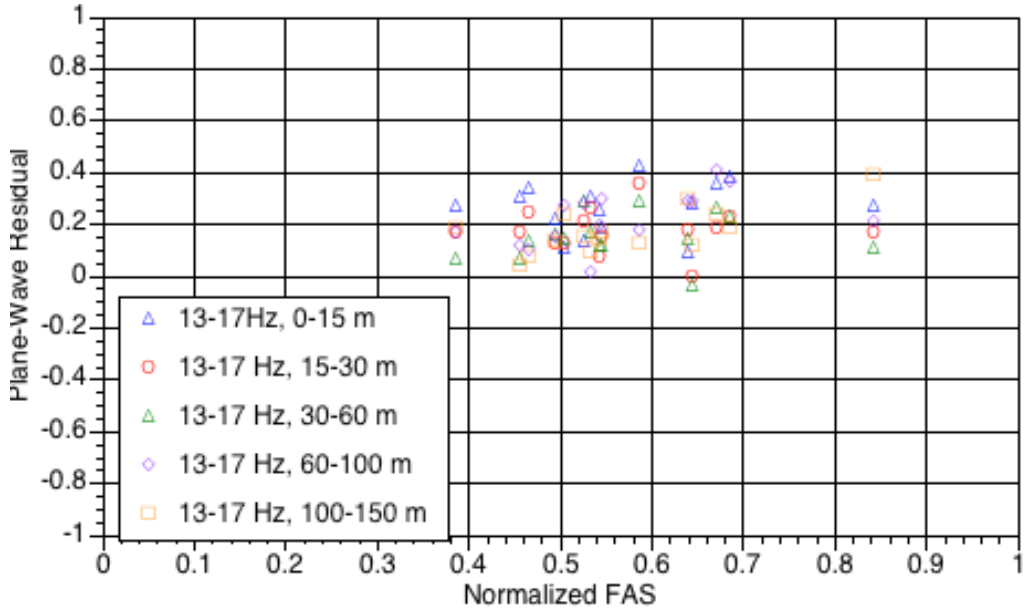

Figure 3-3. Plane-wave residuals for the aligned Pinyon Flat data for 13-17 Hz.

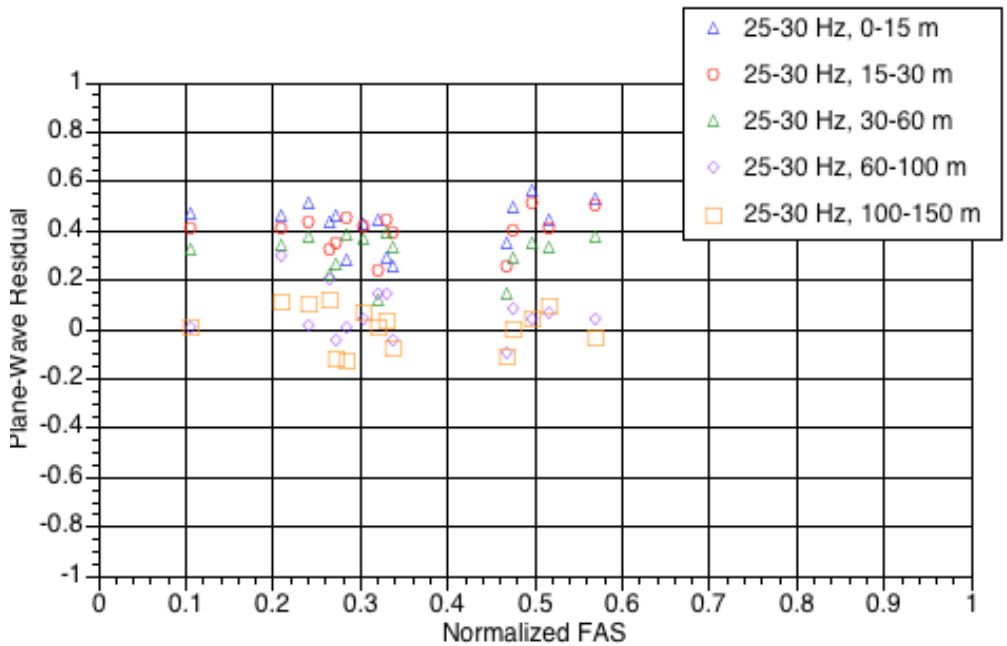

Figure 3-4. Plane-wave residuals for the aligned Pinyon Flat data for 25-30 Hz.

Item 4. Magnitude Dependence of Coherency at High Frequencies

The S2.1 coherency model report (Oct 2006 revision) showed the magnitude dependence of the plane-wave coherency residuals for frequency bands of 3-7 Hz and 8-12 Hz (see Figures 3-5 and 3-6 in the main report). An issue that arose at the Oct 24, 2006 coherency meeting was the possible magnitude dependence at higher frequencies. To evaluate this, the residuals are plotted for frequency bands of 13-17 Hz, and 18-22 Hz. The residuals at the higher do not show a trend with earthquake magnitude, consistent with the lower frequencies

Note: some of the residuals shown in Figures 3-5 and 3-6 in the main report were mislabed as being from separation distances less of 0-15 m and 15-30 m when they were actually from a separation distance of 100-150 m. These mislabled residuals have been corrected in Figures 4-1 to 4-4 shown below.

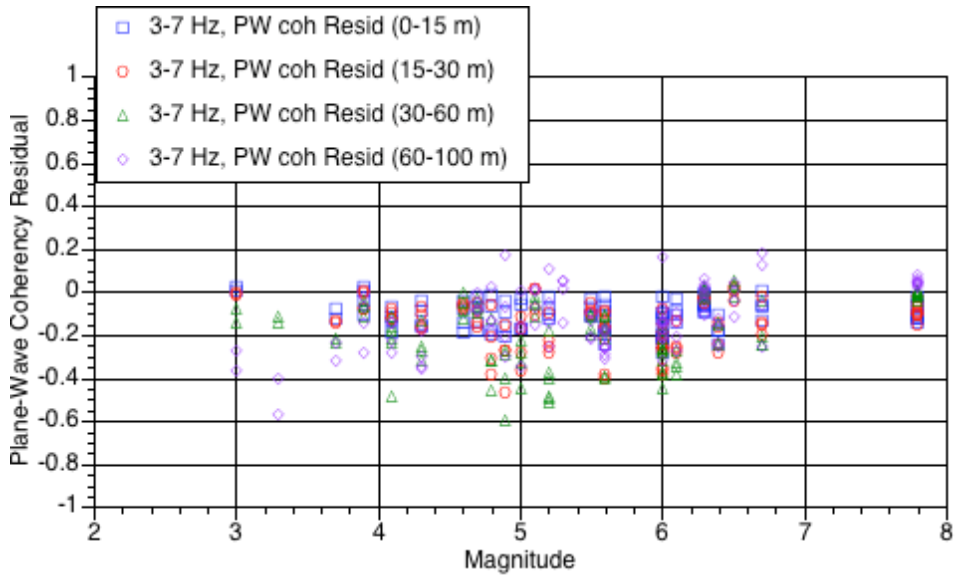

Figure 4-1. Magnitude dependence of plane-wave coherency residuals for 3-7 Hz.

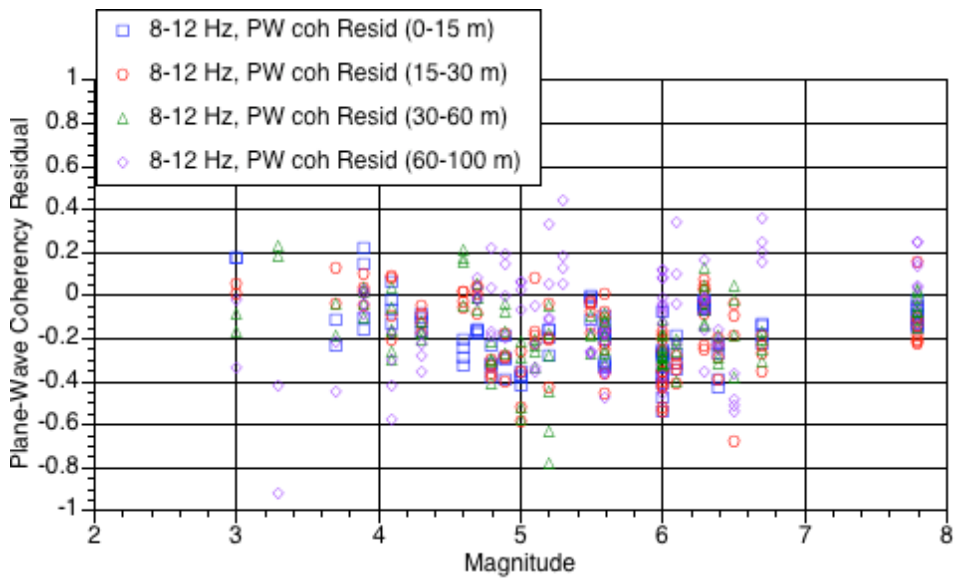

Figure 4-2. Magnitude dependence of plane-wave coherency residuals for 8-12 Hz.

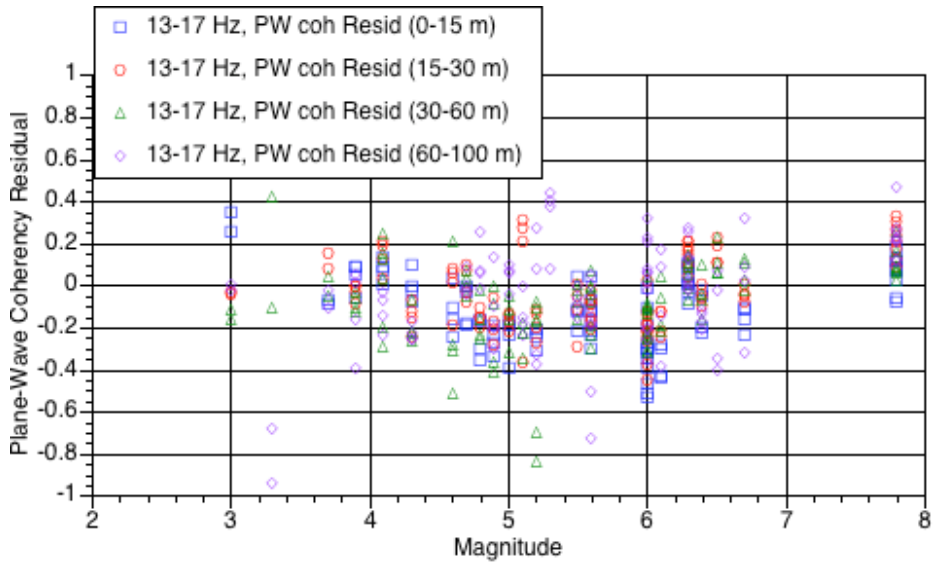

Figure 4-3. Magnitude dependence of plane-wave coherency residuals for 13-17 Hz.

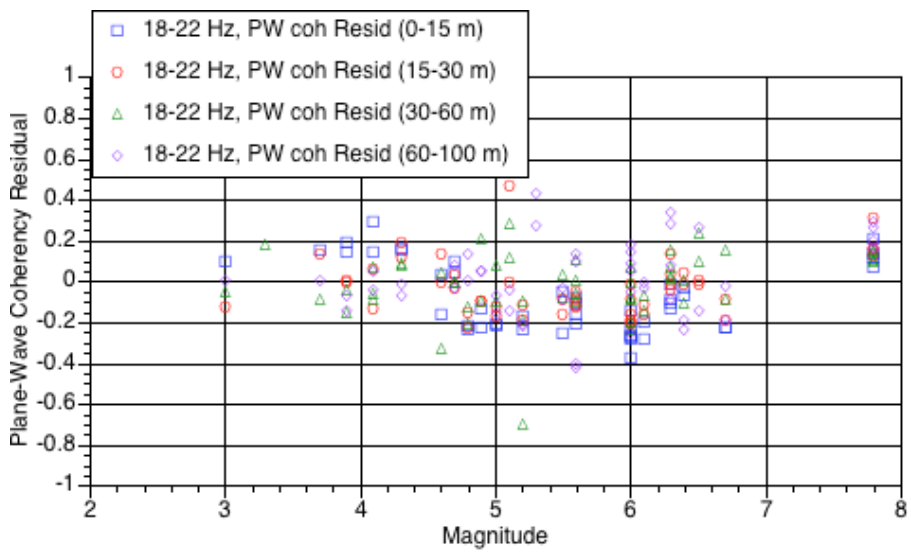

Figure 4-4. Magnitude dependence of plane-wave coherency residuals for 18-22 Hz.

Item 5. High Frequency Coherency from the EPRI Parkfield Array

One issue discussed at the Oct 24, 2006 coherency meeting was the apparent increase in coherency at frequencies above 20 Hz from the EPRI Parkfield data seen in plots from previous studies (See Figure 5-1 below). This was discussed in response to RAI Q5.19. In the response, it was noted that some of the data were at the noise level for frequencies above 20 Hz so that the comparison was not indicative of the high frequency coherency for seismic signals.

Figure 5-1. Comparison of the EPRI Parkfield coherency with the LSST coherency models for (A) 10 m separation and (B) 60 m separation (From Schneider et al, 1990).

At the meeting, it was suggested that the EPRI Parkfield data be evaluated to determine which recordings had signal above the noise at high frequencies and that the high frequency coherency then be computed for these data.

<u>Fourier Spectra</u>
To evaluate the highest frequency at which the data are above the noise, the Fourier amplitude spectra are plotted for the two EPRI Parkfield events. To keep the plots from being too crowed, only five spectra are plotted at a time. In each case, the spectra from the center station (G0) is shown to provide a common reference.

The spectra for Event 1 are shown in Figures 5-1a, b, c and Figures 5-2a,b,c for the EW and NS components respectively. For event 1, the recording from station NE2 EW (Figure 5-1a) reaches the noise level at about 30 Hz, but the other recordings reach the noise level at about 40 to 50 Hz. Therefore, station NE2 EW is excluded.

The spectra for Event 2 are shown in Figures 5-3a, b, c and Figures 5-4a,b,c for the EW and NS components respectively. For this event, the spectra reach the noise level at 25-30 Hz for most stations. Therefore, this event is not used.

<u>Coherency</u>
The plane-wave coherencies computed using the data from EPRI Parkfield event 1 (excluding station NE2 EW) are compared to the plane-wave coherency model given in the main report in Figures 5-5, 5-6, and 5-7 for separation distances of 10-15m, 25-35m, and 50-70m.

At 10-15m separation, for frequencies above 20 Hz, the NS component has average coherencies greater than the model, but for the EW component, the average coherency is consistent with the model.

At 25-35 m separation, a similar trend is seen, but in this case the EW component has coherencies that tend to be above the model above 20 Hz, but the coherencies from the NS component are now consistent with the model above 20 Hz.

At 50-70 m separation, both components have coherencies above 20 Hz that are consistent with the model.

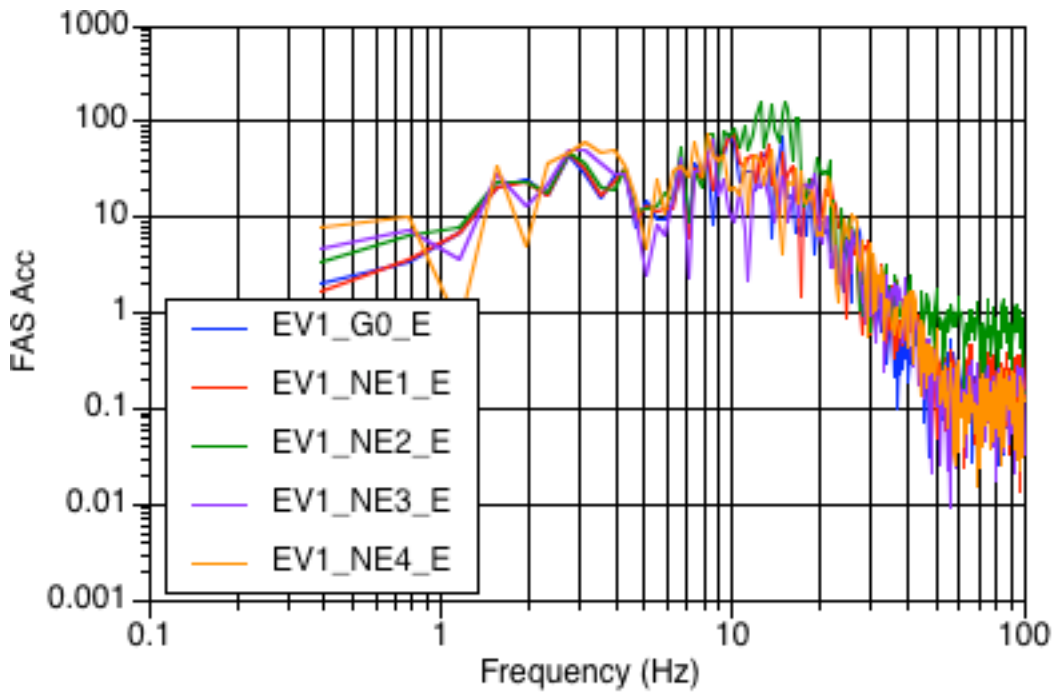

Figure 5-1a. Spectra for EPRI Parkfield, Event 1, EW

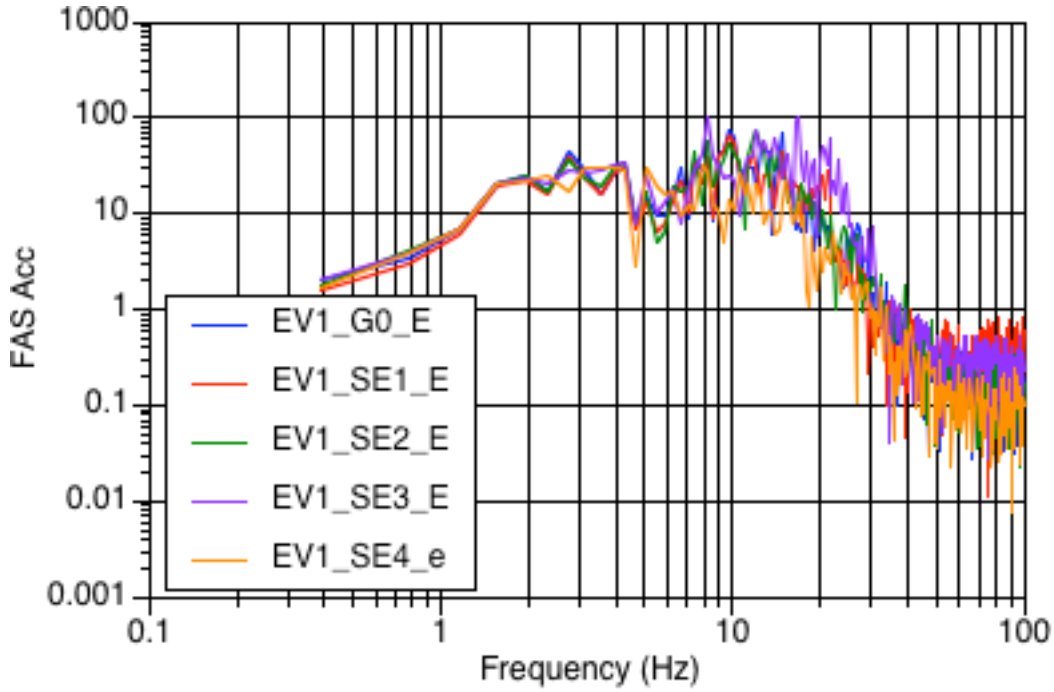

Figure 5-1b. Spectra for EPRI Parkfield, Event 1, EW

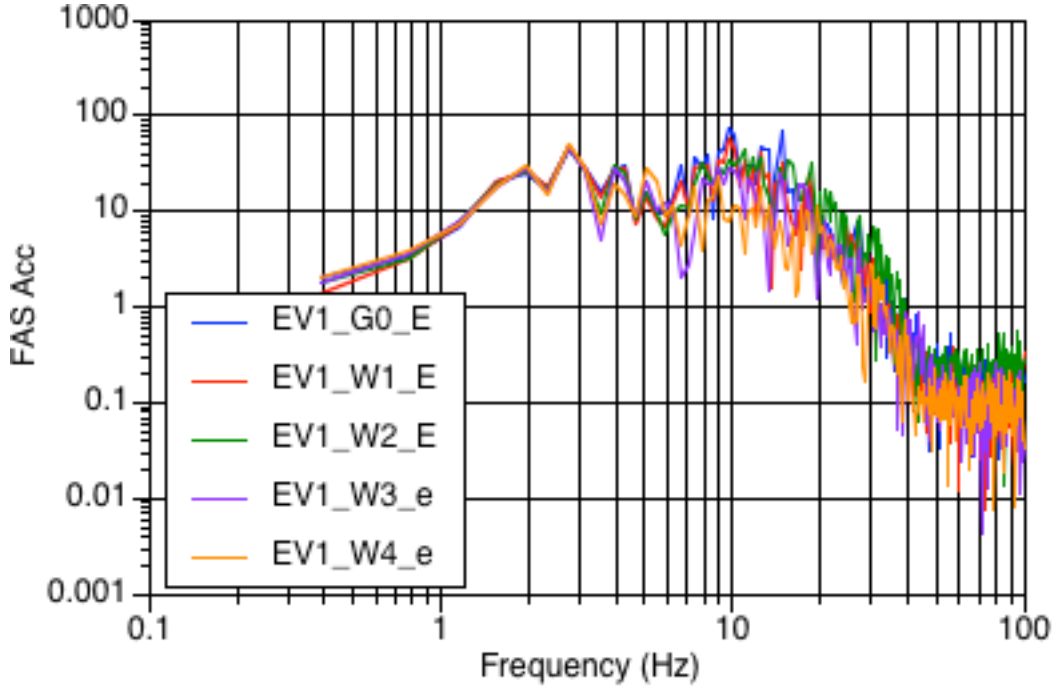

Figure 5-1c. Spectra for EPRI Parkfield, Event 1, EW

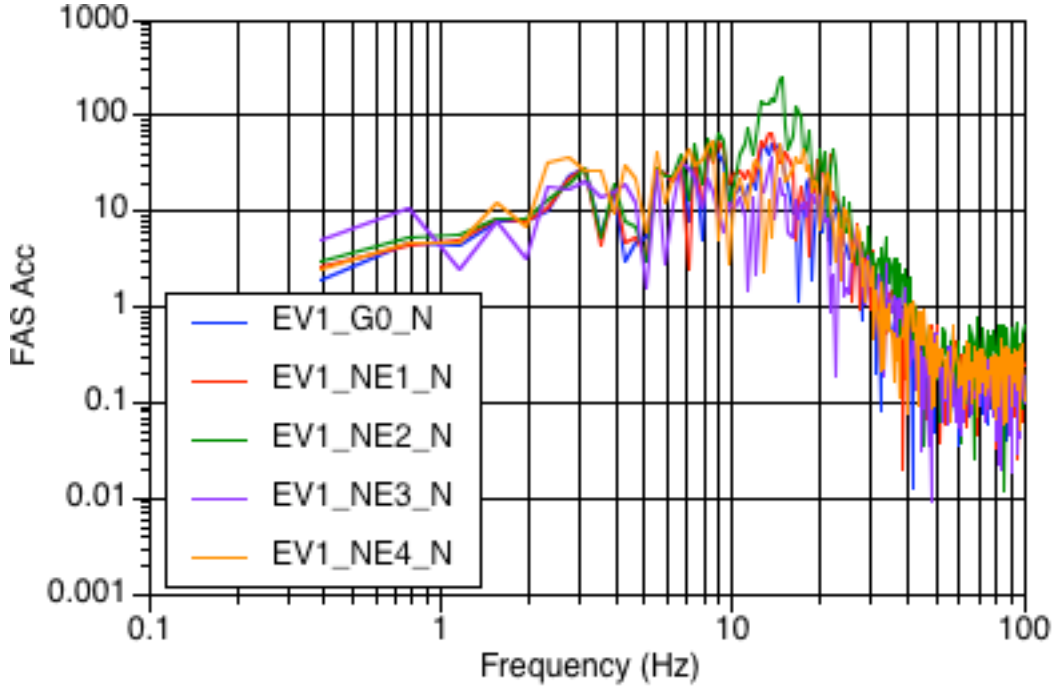

Figure 5-2a. Spectra for EPRI Parkfield, Event 1, NS

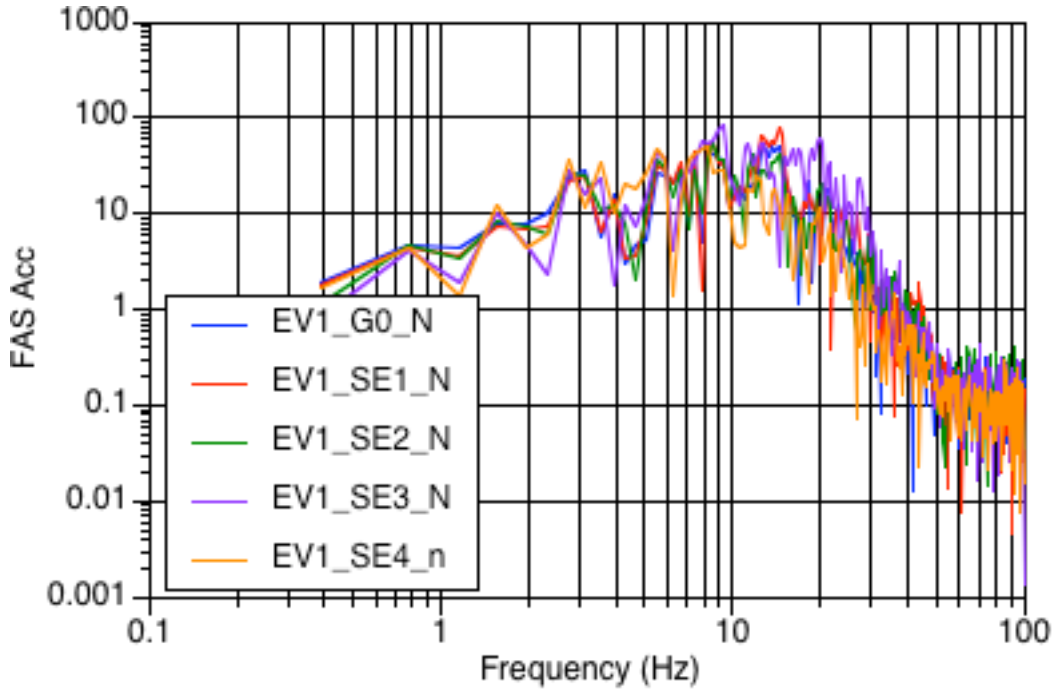

Figure 5-2b. Spectra for EPRI Parkfield, Event 1, NS

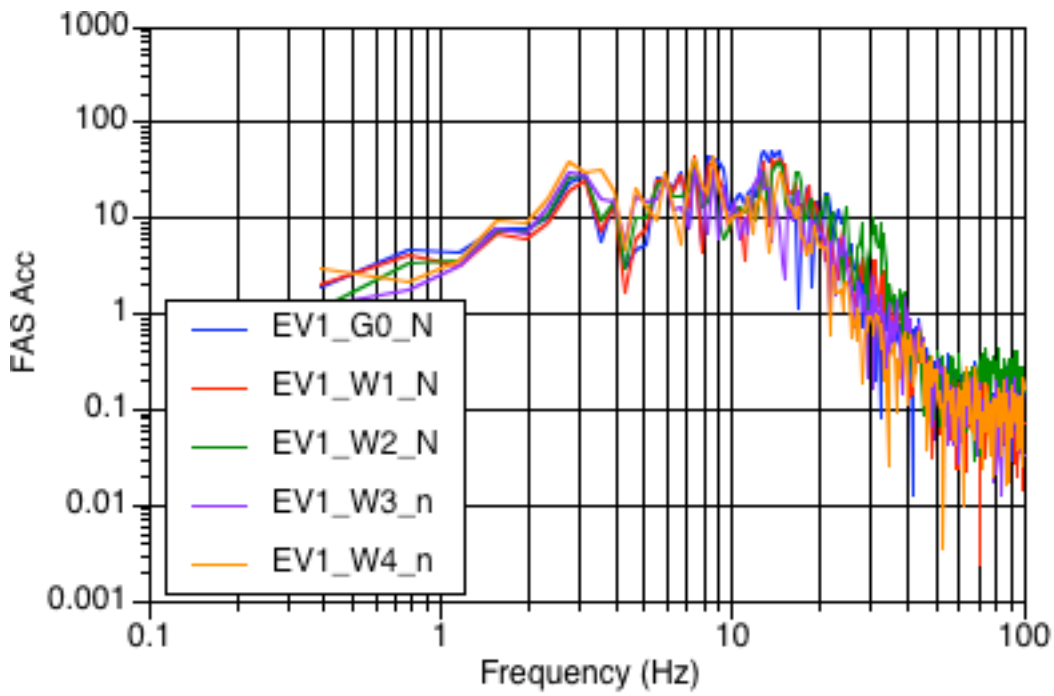

Figure 5-3c. Spectra for EPRI Parkfield, Event 1, EW

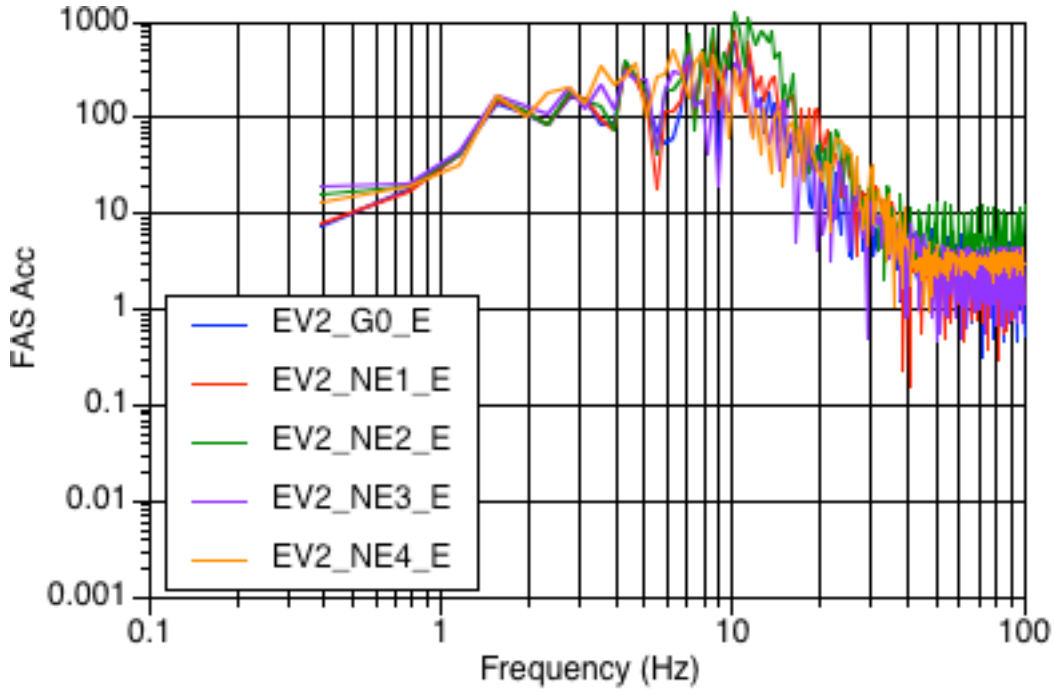

Figure 5-3a. Spectra for EPRI Parkfield, Event 2, EW

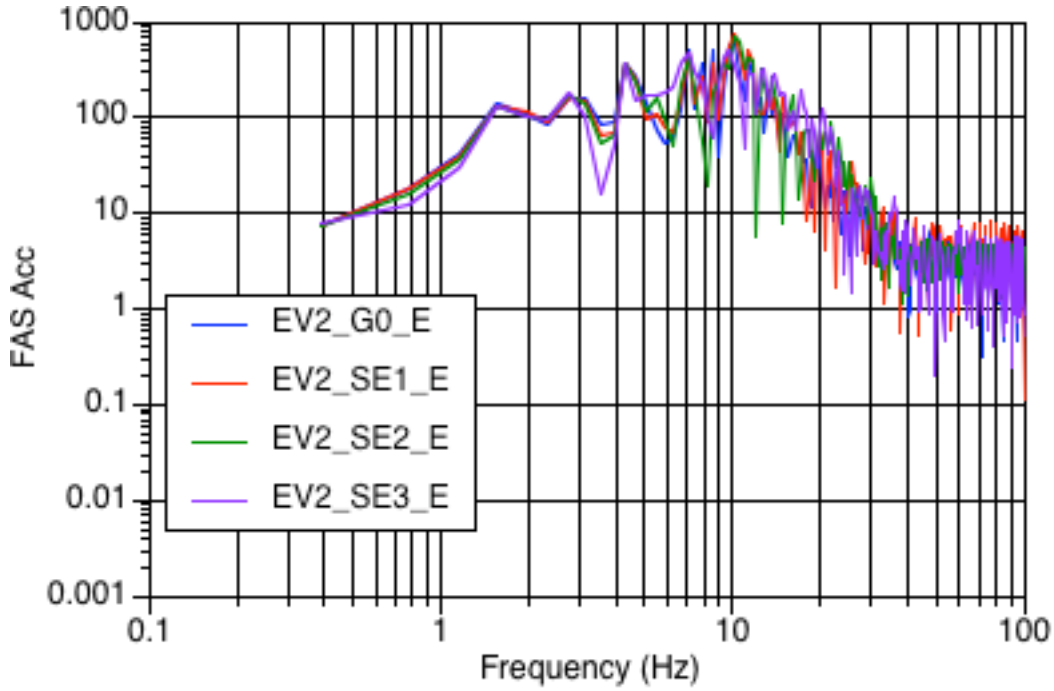

Figure 5-3b. Spectra for EPRI Parkfield, Event 2, EW

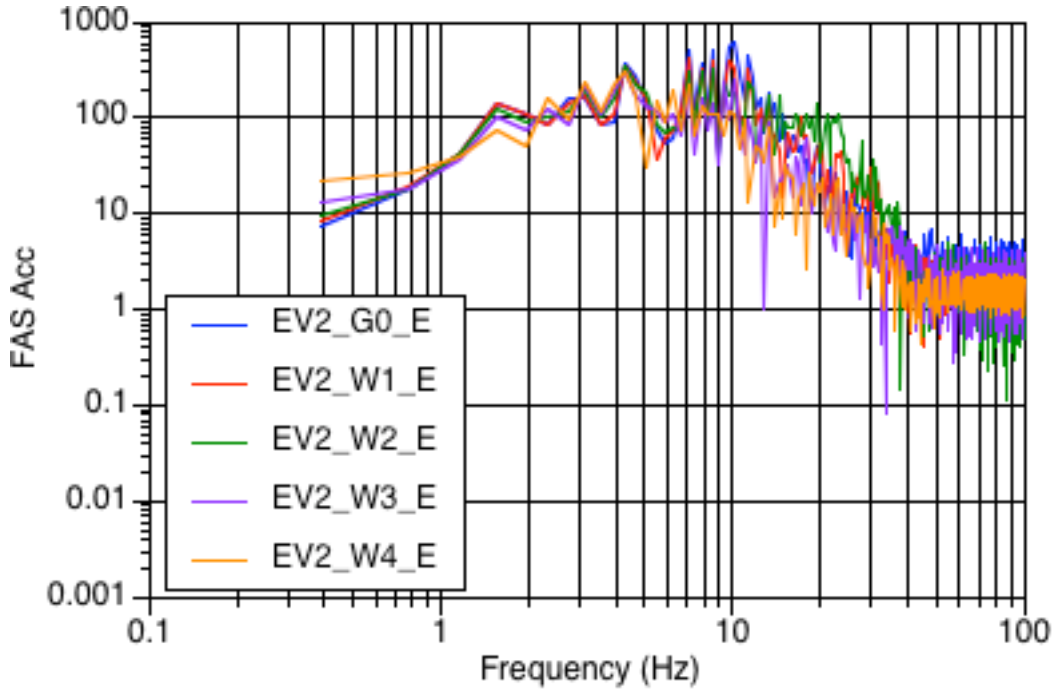

Figure 5-3c. Spectra for EPRI Parkfield, Event 2, EW

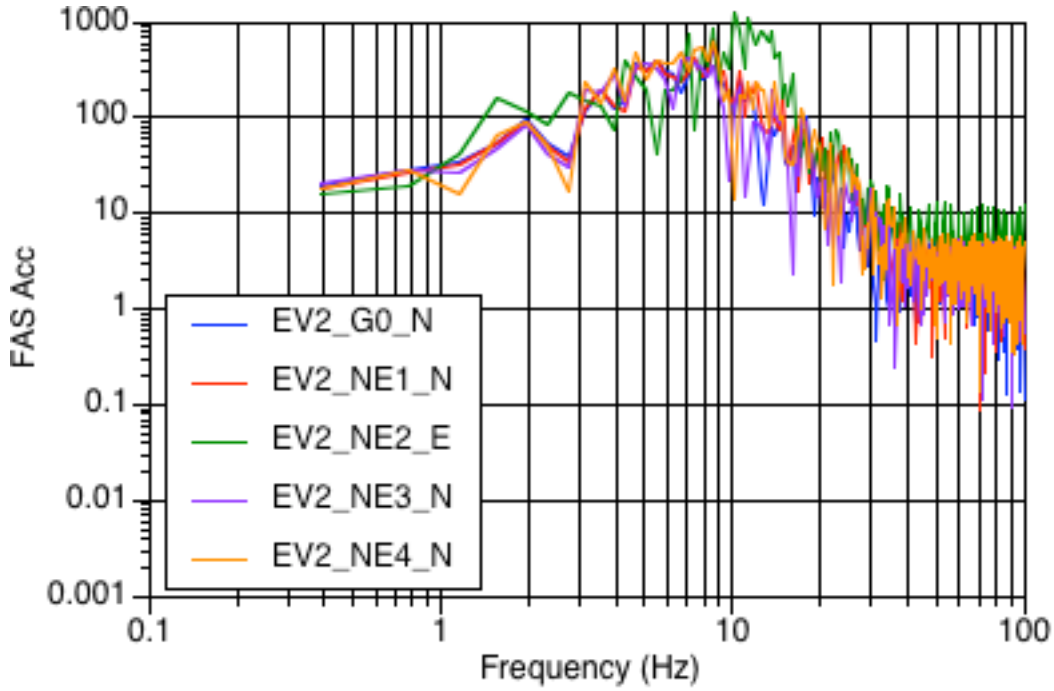

Figure 5-4a. Spectra for EPRI Parkfield, Event 2, NS

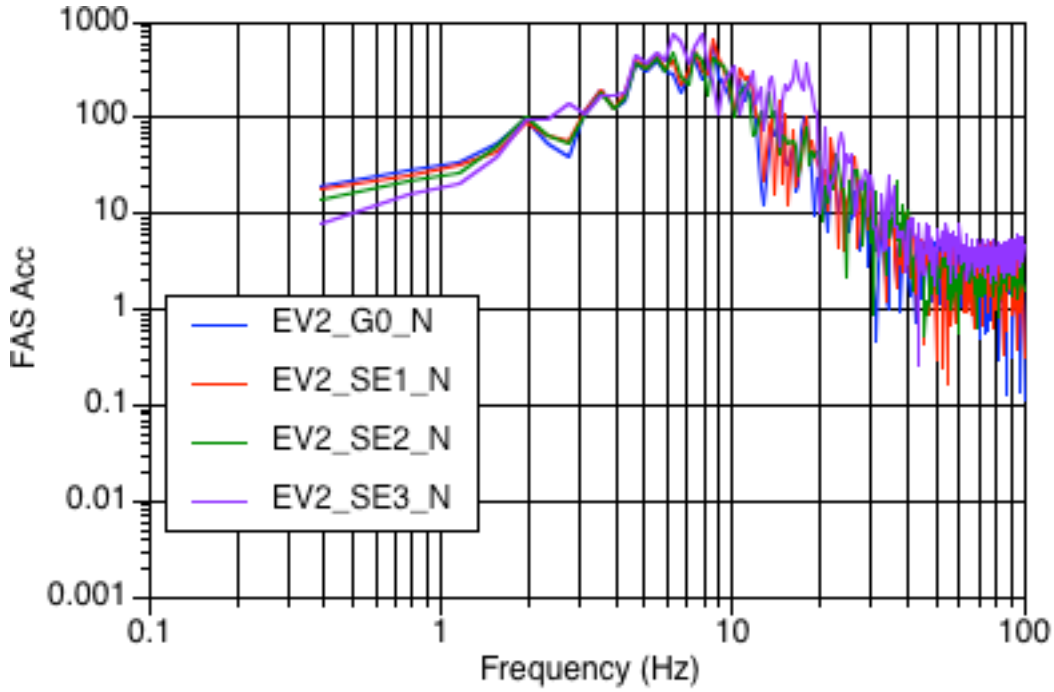

Figure 5-4b. Spectra for EPRI Parkfield, Event 2, NS

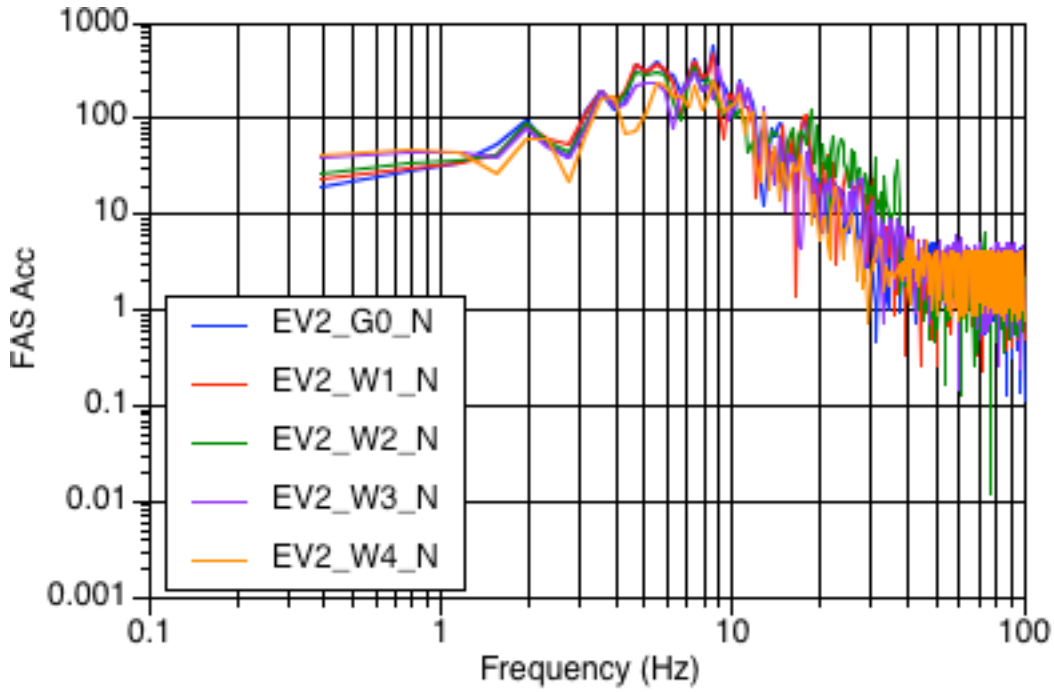

Figure 5-4c. Spectra for EPRI Parkfield, Event 2, NS

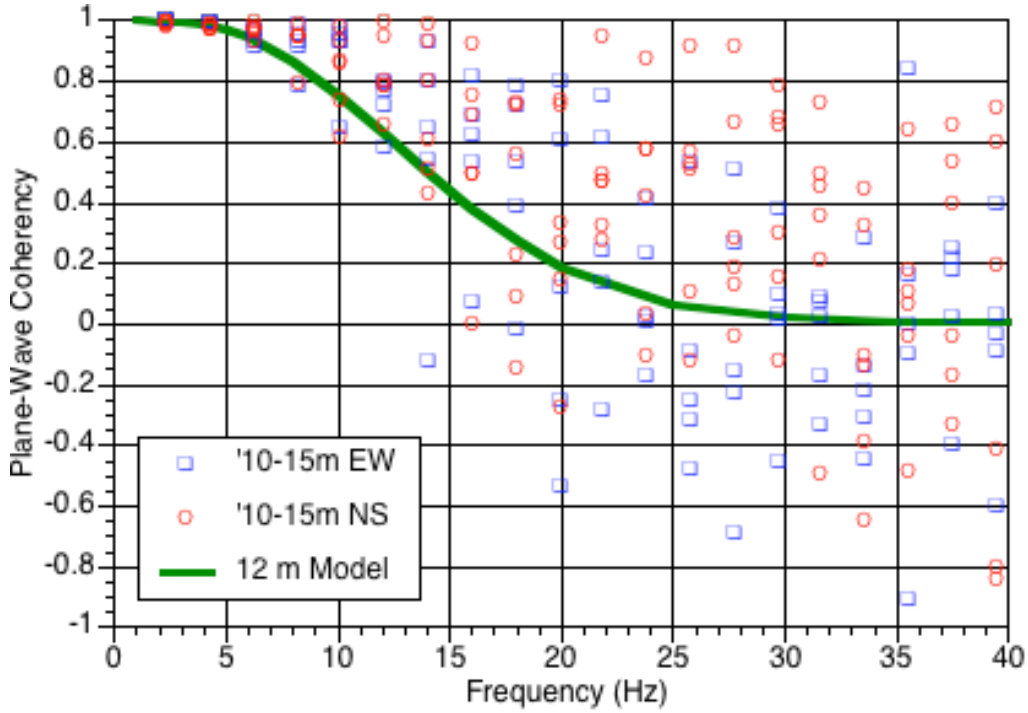

Figure 5-5. Comparison of the plane-wave coherency from EPRI Parkfield Event 1 to the median model

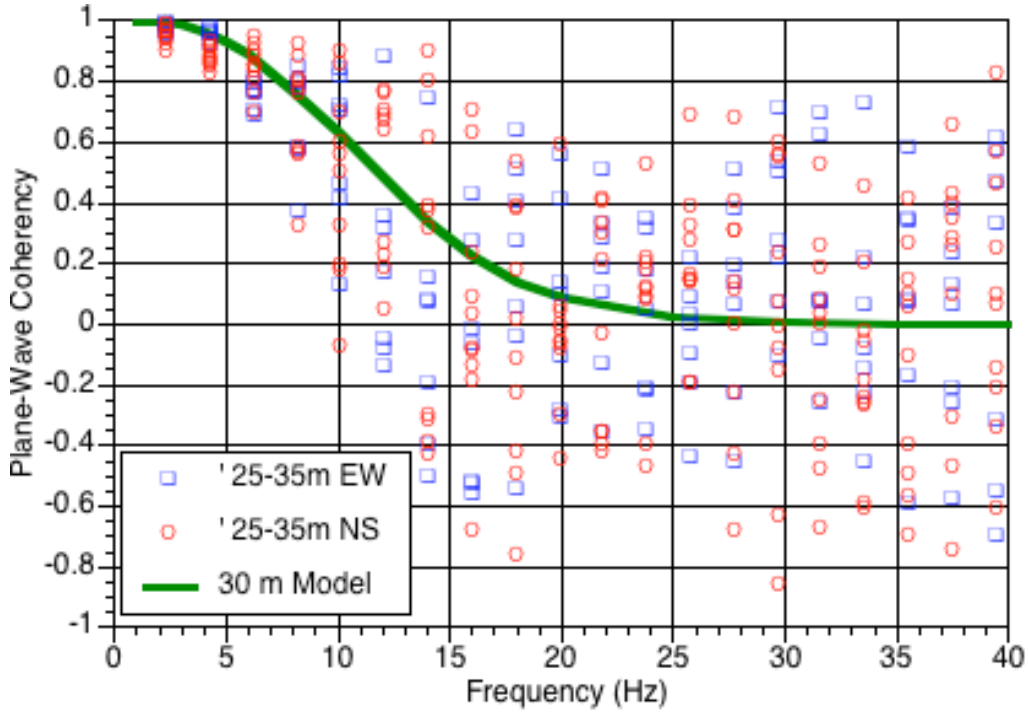

Figure 5-6. Comparison of the plane-wave coherency from EPRI Parkfield Event 1 to the median model

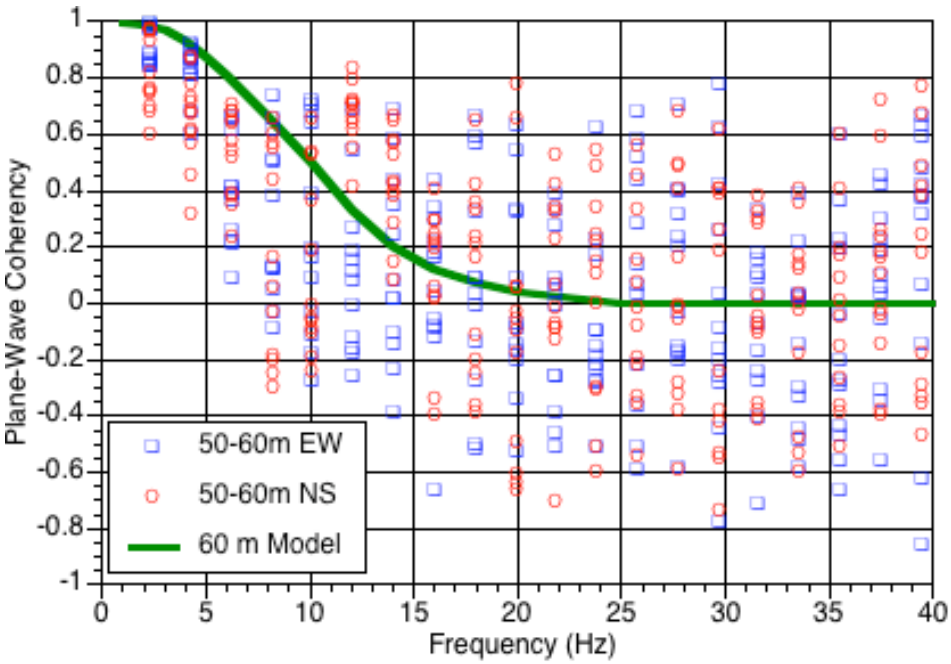

Figure 5-7. Comparison of the plane-wave coherency from EPRI Parkfield Event 1 to the median model